University of Massachusetts Lowell

Department of Environmental, Earth, and Atmospheric Sciences

Scientific Report No. 060301

Total Internal Partition Sums for Molecular Species on the 2000 Edition of the HITRAN Database

J. Fischer[a], R.R. Gamache[a†], A. Goldman[b], L.S. Rothman[c], and A. Perrin[d]

[a]*Department of Environmental, Earth, and Atmospheric Sciences, University of Massachusetts Lowell, Lowell, MA 01854, U.S.A.*

[b]*Department of Physics, University of Denver, Denver, CO 80208, U.S.A.*

[c]*Harvard-Smithsonian Center for Astrophysics, 60 Garden St, Cambridge, MA 02138 USA*

[d]*Laboratoire de Photophysique Moléculaire, Université Paris Sud, 91405 Orsay, FRANCE*

† Corresponding author. Email address: Robert_Gamache@uml.edu

Abstract

Total internal partition sums (TIPS) are calculated for all molecular species in the 2000 HITRAN database. In addition, the TIPS for 13 other isotopomers/isotopologues of ozone and carbon dioxide are presented. The calculations address the corrections suggested by Goldman et al. (J. Quant. Spectrosc. Radiat. Transfer 66 (2000) 455). The calculations consider the temperature range 70-3000 K to be applicable to a variety of remote sensing needs. The method of calculation for each molecular species is stated and comparisons with data from the literature are made whenever possible. A new method of recall for the partition sums, Lagrange 4-point interpolation, is developed. This method, unlike previous versions of the TIPS code, allows all molecular species to be considered. Convergence of the partition sums as a function of temperature, analytical modeling of the rotational partition sum, and the quality of the recalculated quantities are discussed.

Overview

The aim of this work has been to provide a comprehensive set of total internal partition sums (TIPS) for species of atmospheric interest, calculated to the greatest possible degree of accuracy and packaged in a form that allows for easy and rapid recall of the data. This work is therefore a modern revision of previous calculations which supplants previously released partition function data. As such, the work is based upon prior work by Gamache et al. [1,2] and incorporates all of the corrections discussed in Goldman et al. [3], as well as newer physical constants and molecular parameters.

Since one of the many uses of the partition is for application to retrievals from remotely sensed data, these partition functions are provided as a companion to the HITRAN 2000 spectroscopic database [4]. Therefore, the scope of the calculations matches these interests. Partition functions are provided for all molecular species and isotopomers present on the HITRAN database, except for the O atom, for which rotational and vibrational partition functions are undefined. Additionally, partition functions are provided for a number of ozone species which are not currently on the HITRAN database. The temperature range of the calculations (70-3000K) was selected to match a variety of remote sensing needs (planetary atmospheres, combustion gases, plume detection, etc.). Although there are a number of molecular species for which the partition sum at high temperatures is of no practical importance at present, e.g. ozone, hydrogen peroxide, the aim was to have a consistent set of partition sums for all molecular species.

Methodology

The general methodology used in this study was selected to minimize the possibility of human error or faulty constants producing error in the final partition sums. Molecular constants used were taken from scientific literature. The total internal partition sum is given by a sum over all states, *s*, labeled by the electronic, vibrational, rotational, torsional, … structure of the molecule,

$$Q(elec, vib, rot, tors, etc) = d_i \sum_{all\ states\ s} d_s\ e^{-E_s / kT} \qquad (1)$$

where d_i is the state-independent degeneracy factor and d_s is the state-dependent degeneracy factor (see below and [2]) and E_s is the energy of the electronic, vibrational, rotational, torsional, etc. state. In practice, the energy states are usually not known for all rotational levels of all vibrational states of all electronic states. When there are other complications, such as lamda doubling, torsional motion, etc. the situation for the energy states is more complex. In such cases it is assumed that

$$E(elec, vib, rot, tors, ...) = E_{elec} + E_{vib} + E_{rot} + E_{tors} + \bullet\bullet\bullet \qquad (2)$$

from which the product approximation can be made

$$Q(elec, vib, rot, tors, etc) = Q_{elec} \times Q_{vib} \times Q_{rot} \times Q_{tors} \times \bullet\bullet\bullet \qquad (3)$$

The problem is now reduced to calculating the electronic, vibrational, rotational, … partition sums. Which approach is used is determined by the availability of energy states for the molecule in question.

For the rotational partition sums, when possible, rotational energy levels were calculated from these constants using appropriate expressions and compared to measured energy levels. For certain species, energy levels were provided by other researchers. These energy levels were then used to evaluate the rotational partition sum at a variety of temperatures by direct summation of the expression:

$$Q_{rot} = d_i \sum_{\substack{all \\ rotational \\ states}} d_r \, e^{-E_r / kT} \tag{4}$$

where d_r is the degeneracy of the rotational state with energy E_r. This sum clearly becomes divergent at high enough temperatures for a given set of energies. Therefore, the convergence of these partition sums was tested by plotting $Q_{rot}(T, J)$ versus the rotational quantum number J at various temperatures of interest. Converged partition sums exhibit a horizontal asymptote at energy levels where E_r is significantly larger than kT cease to contribute significantly to the sum. Non-converged partition sums do not exhibit this asymptote. By finding the greatest temperature at which these convergence plots still exhibited an asymptote, it was possible to determine the highest temperature to which a direct sum could be used for a given set of energies.

Next, an appropriate analytical expression was used to evaluate $Q_{rot}(T)$. The expression used was selected based on molecular symmetry. For linear molecules, McDowell's expression was used [5]; for asymmetric rotors, Watson's expression was used [6] and for spherical [7, 8] and symmetric top molecules [9], McDowell's expressions were used.

A comparison was then performed between the direct sum and the analytical expression for each species. Bearing in mind that the direct sum is only accurate at temperatures low enough for it to remain converged and that all of the analytical expressions used are approximations which become better in the limit of high temperatures, the assumption was made that if a good agreement can be demonstrated between a converged direct sum and an analytical expression for a fair temperature range, that the analytical expression probably exhibits similar or smaller errors at greater temperatures. In all cases, a good agreement could be demonstrated between the two methods and, in most cases, the analytical expression was used for the entire temperature range. For certain species where the analytical expression did not work as well for lower temperatures, the direct sum was used for low temperatures and an analytical expression was used for higher temperatures.

For all species, unless otherwise noted, the vibrational partition function was calculated using the harmonic oscillator approximation of Herzberg [10]. Vibrational fundamentals were taken from the literature and used in the following expression:

$$Q_{vib}(T) = \prod_{vibrational\ fundamentals} \frac{1}{1 - e^{hcE_\nu / kT}} \tag{5}$$

Once the vibrational and rotational partition functions were calculated for species in the electronic ground state and with no other structure (hyperfine, torsion, …), the product approximation, Q_{vib} x $Q_{rot,}$ was used to evaluate the total internal partition functions. The product approximation assumes that the vibrational and rotational energy levels are totally independent of each other and therefore, that the rotational and vibrational partition functions are also totally independent. With this approximation, the total internal partition function, for most molecules, is merely the product of the rotational and vibrational partition functions. The validity of the product approximation was tested in a rough manner by comparing the total internal partition function for CO_2 calculated by using the product approximation with an analytical expression with a partition function calculated by a direct sum of ro-vibrational energy levels. The results of this test are summarized in Fig. 1.

One often neglected aspect of calculating partition sums is the inclusion of state independent degeneracy factors. Degeneracy factors can be divided into state dependent and state independent components. Note, below, when the state dependent degeneracy factors are discussed here it is the factor in addition to the normal ($2J+1$) or the ($2F+1$) factor. These additional state dependent degeneracy factors occur in systems in which the rotational wavefunction of the species couples with the nuclear wavefunctions of some of the atoms in the molecule. Typically, this happens in species with some degree of symmetry where only certain products of rotational and nuclear wavefunctions yield the proper symmetry for the complete wavefunctions. The net result of this is that for some

molecules, even and odd symmetry states have different weights and these values must be factored in accordingly when calculating partition sums.

For molecules where two identical nuclei are exchanged upon rotation, it is easy to determine the nuclear statistical weights which are part of the state dependent degeneracy factors. For Fermi systems (i.e. molecules where the exchanged nuclei have half-integer spins) and Bose systems (i.e. molecules where the exchanged nuclei have integer spins) the following equations give the state dependent degeneracy factors:

$$\begin{array}{ll} Fermi\ system-even: & \frac{1}{2}[(2I_x+1)^2-(2I_x+1)] \\ Bose\ system-odd: & \end{array}$$

$$\begin{array}{ll} Fermi\ system-odd: & \frac{1}{2}[(2I_x+1)^2+(2I_x+1)] \\ Bose\ system-even: & \end{array} \tag{6}$$

where I_x is the nuclear spin of the atoms which are interchanged. For example, for H_2O, the two interchanged nuclei are the hydrogen atoms, which are spin ½. Inserting this value into the above equations gives a three-fold degeneracy for the odd states and a one-fold degeneracy for the even states. For $^{16}O_3$, the two interchanged nuclei are oxygen atoms with spin zero. Substituting this value into the above equations yields a one-fold degeneracy for the even levels and a zero-fold degeneracy for the odd levels (i.e., such levels do not exist). For molecules which have more than one pair of atoms exchanged upon rotation, expressions for the number of spin functions for each state are given in Ref. 10, p17, Eqs. (I.8) and (I.9).

When direct sums were calculated in this work, state dependent factors were handled explicitly by calculating the parity of each state using an expression appropriate for the molecular symmetry of the species involved and the correct degeneracy factors were incorporated into the direct sum. When analytical expressions were used, an average state dependent factor was used by taking the arithmetic mean of the state dependent factors involved. For example, for $^{16}O_3$, a factor of 0.5 was used to account for the total of the state dependent factors.

State independent factors are often omitted from partition sum calculations. They are, however, necessary for the partition functions to relate to thermodynamic quantities. State independent factors occur in species where there are atoms which have non-zero spins and which are not interchanged upon rotation. This degeneracy factor is expressed as $\prod(2I+1)$, where I is the nuclear spin and the product is taken over all nuclei not interchanged by rotation. [10] Note, there are other factors that can sometimes mimic state independent factors, for example a doubling for all levels when there is lambda doubling, torsion or inversion. These factors are discussed specifically in the appropriate sections of the text.

Although the state independent factors are often omitted in studies which report partition sums, it is usually not a problem, since the actual values of the partition sum are infrequently used. More commonly, a ratio of partition sums is used. This causes the state independent factors to cancel out. However, in this study, every attempt has been made to include the complete state independent factor for all species and hence determine the true total internal partition function. In comparing the partition sums from this study to others from the literature, it is sometimes necessary to multiply by an integer value to

obtain agreement due to the omission of certain factors in other studies. Such comparisons are discussed specifically in the text.

CALCULATIONS

H_2O

Six isotopomers of H_2O were considered in this study: $H_2{}^{16}O$, $H_2{}^{18}O$, $H_2{}^{17}O$, $HD^{16}O$, $HD^{18}O$ and $HD^{17}O$. For the principal species, the rotational energy levels are those of Coudert [11]. In all other cases, rotational energy levels were calculated by diagonalizing the Watson Hamiltonian [12] with appropriate constants [13]. The state independent factors contributing to the partition function were 1, 1, 6, 6, 6 and 36 for $H_2{}^{16}O$, $H_2{}^{18}O$, $H_2{}^{17}O$, $HD^{16}O$, $HD^{18}O$ and $HD^{17}O$, respectively. The state dependent factors due to the coupling of the nuclear and rotational wavefunctions were a 3-fold weighting for odd states and a 1-fold weighting for even states in those species with C_{2v} symmetry (i.e. $H_2{}^{16}O$, $H_2{}^{18}O$, $H_2{}^{17}O$). The evenness/oddness of the state is determined by the parity of $(Ka-Kc+n\nu_3)$, where $n\nu_3$ is the number of vibrational quanta in the ν_3 mode (asymmetric stretch). Direct sums of Q_{rot} converged up to about 900K, 1600K, 1200K, 1200K, 75K and 75K for $H_2{}^{16}O$, $H_2{}^{18}O$, $H_2{}^{17}O$, $HD^{16}O$, $HD^{18}O$ and $HD^{17}O$, respectively.

The analytical expression of Q_{rot} used for H_2O was that of Watson [6], with the constants of Ref. 13. At points within the temperature range of interest for which the direct sum remained converged, the greatest differences between the direct sum and the analytical expression were 0.80%, 2.1%, 3.0% and 1.0% for $H_2{}^{16}O$, $H_2{}^{18}O$, $H_2{}^{17}O$, $HD^{16}O$ respectively. Comparisons were not made for the other isotopomers due to the very

limited number of energy levels available for the direct sum. Figure 2 shows the difference between the direct sum and the analytical expression for the $H_2{}^{16}O$ species. The figure shows that the difference between the two methods is quite large at very low temperatures, where the analytical expression is unable to properly model the quantum structure of the system. The difference is also quite large at high temperatures, where the direct sum no longer converged. However, at intermediate temperatures, there is a region where the agreement between the two methods is quite good. In order to provide the most accurate representation of the partition sum, a combination of the direct sum and the analytical expression was used for the final partition sums for the four most abundant species. In part, this method was selected because the greatest errors for all of these species occurred at low temperatures, where the analytical expression could not properly model the fine quantum structure of the molecule. The lowest temperatures at which the analytical expression was used were 1401K, 451K, 349K and 674K for $H_2{}^{16}O$, $H_2{}^{18}O$, $H_2{}^{17}O$, $HD^{16}O$ respectively. At these temperatures, the differences between the direct sum and the analytical expression were 0.62%, 0.52%, -0.46% and 0.66% for $H_2{}^{16}O$, $H_2{}^{18}O$, $H_2{}^{17}O$, $HD^{16}O$, respectively.

The vibrational partition sums were calculated using the vibrational fundamentals of Ref. [14] and are presented in Table 1

The values of the partition sums calculated for H_2O in this study agree quite well with calculations from other sources. For example, for the principal species, we obtained values for the rotational partition function of 63.69, 174.56, 178.09 and 294.57 at 150K, 296K, 300K and 420K. These values compare well with the values of 63.68, 174.6, 178.12 and 295.6 from Refs. 15, 16, 15, and 16, respectively.

CO_2

Nine isotopomers of CO_2 were considered in this study: $^{12}C^{16}O_2$, $^{13}C^{16}O_2$, $^{12}C^{16}O^{18}O$, $^{12}C^{16}O^{17}O$, $^{13}C^{16}O^{18}O$, $^{13}C^{16}O^{17}O$, $^{12}C^{18}O_2$,$^{12}C^{17}O^{18}O$, and $^{12}C^{17}O_2$. For $^{12}C^{16}O_2$, $^{13}C^{16}O_2$, and $^{12}C^{16}O^{18}O$, the energy levels used were those of Rothman et al. [17]. For the remaining species, except $^{12}C^{17}O_2$, the energy levels were calculated using the constants of Chedin and Teffo [18]. For $^{12}C^{17}O_2$ the partition sums were only done by analytical formula. State dependent factors for symmetric species were calculated using basic spectroscopic rules, resulting in a 1-fold degeneracy for even levels and a 0-fold degeneracy for odd levels (i.e., such levels do not exist). State independent factors of 1, 2, 1, 6, 2, 12, 1, 6 and 1 were used for species $^{12}C^{16}O_2$, $^{13}C^{16}O_2$, $^{12}C^{16}O^{18}O$, $^{12}C^{16}O^{17}O$, $^{13}C^{16}O^{18}O$, $^{13}C^{16}O^{17}O$, $^{12}C^{18}O_2$, $^{12}C^{17}O^{18}O$, and $^{12}C^{17}O_2$ respectively. Direct sums, Q_{rot}, converged up to about 1800K, 1300K, 1200K, 600K, 700K, 700K, 500K and 600K for species $^{12}C^{16}O_2$, $^{13}C^{16}O_2$, $^{12}C^{16}O^{18}O$, $^{12}C^{16}O^{17}O$, $^{13}C^{16}O^{18}O$, $^{13}C^{16}O^{17}O$, $^{12}C^{18}O_2$ and $^{12}C^{17}O^{18}O$, respectively.

The analytical expression used for CO_2 was that of McDowell [5]. The constants used for the analytical expression were those of [18]. Comparisons between the direct sum and the analytical expression had the greatest differences at points for which the direct sum remained converged within the temperature range of interest of 0.49%, 0.34%, 0.91%, 0.59%, 0.70%, 0.70%, 0.49% and 0.59% for species $^{12}C^{16}O_2$, $^{13}C^{16}O_2$, $^{12}C^{16}O^{18}O$, $^{12}C^{16}O^{17}O$, $^{13}C^{16}O^{18}O$, $^{13}C^{16}O^{17}O$, $^{12}C^{18}O_2$ and $^{12}C^{17}O^{18}O$, respectively. For all species, the analytical expression was used throughout the entire temperature range.

The vibrational partition sums were calculated using the constants of [18] and are given in Table 2.

Comparison with other published values shows good agreement. Our values of the total internal partition sum at 300K are 291.89, 588.57, 620.08, 3614.29 and 1250.77 for $^{12}C^{16}O_2$, $^{13}C^{16}O_2$, $^{12}C^{16}O^{18}O$, $^{12}C^{16}O^{17}O$, $^{13}C^{16}O^{18}O$ respectively. These compare favorably with the values of Gray and Young [19], which are 291.05, 293.40, 618.41, 600.65 and 623.58 after factoring in the state independent factors of 1, 2, 1, 6 and 2 respectively.

O_3

All eighteen isotopomers of ozone are considered in this study. Rotational energy levels were derived using the constants from Flaud et al. [20] for the principal isotopomer $^{16}O_3$, Flaud et al. [21] for isotopomers $^{16}O^{16}O^{18}O$, $^{16}O^{18}O^{16}O$, $^{18}O^{16}O^{18}O$, $^{18}O^{18}O^{16}O$ and $^{18}O_3$, Rinsland et al. [22] for isotopomers $^{16}O^{17}O^{16}O$ and $^{16}O^{16}O^{17}O$, and the rotational constants of Barbe [23] for all other species. The state-dependent and state-independent degeneracy factors are listed in Table 3. Direct sums of Q_{rot} converged up to about 1800K, 500K, 400K, 500K and 500K for species $^{16}O_3$, $^{16}O^{16}O^{18}O$, $^{16}O^{18}O^{16}O$, $^{18}O^{18}O^{16}O$ and $^{18}O^{16}O^{18}O$ respectively. Figure 3 is a convergence plot for the $^{16}O_3$ species. The general trend of all convergence plots is similar to this graph. For a given temperature, lower rotational energy levels contribute significantly more to the partition sum, due to the $e^{-E_s/kT}$ term. At a constant temperature, as higher rotational levels are summed, they contribute less and less to the total internal partition function and a horizontal

asymptote is seen in the graph. However, at higher temperatures, it is impossible to reach this point with a finite set of rotational energy levels. The highest temperature at which the graph still exhibits a horizontal asymptote (i.e. the point where summation of all higher energy levels leads to a negligible change in the total value of the partition sum) is the highest temperature at which the partition sum remains converged.

The analytical expression used for Q_{rot} was that of Watson [6]. The constants used for the analytical expression were the same as those used to obtain energy levels as given above. A comparison of the direct sum with the analytical expression revealed that the greatest differences at points for which the direct sum remained converged within the temperature range of interest were 9.10%, 0.42%, 0.32%, 4.90% and 0.42% for species $^{16}O_3$, $^{16}O^{16}O^{18}O$, $^{16}O^{18}O^{16}O$, $^{18}O^{18}O^{16}O$ and $^{18}O^{16}O^{18}O$ respectively. Comparisons were not performed for the other species due to the small number of rotational energy levels available. Partition sums evaluated by analytical expression were used for all species at all temperatures.

The vibrational fundamentals used for species $^{16}O_3$, $^{16}O^{16}O^{18}O$ and $^{16}O^{18}O^{16}O$ are those of Refs. [14, 21, 24, 25], those for species $^{16}O^{17}O^{16}O$ and $^{16}O^{16}O^{17}O$ are from Refs. [22, 26], while the fundamentals used for all other species are those of Barbe [23]. These are presented in Table 4.

Partition sums for ozone agree quite well with other calculations. Recent review calculations performed by Flaud (private communication) and cited in Goldman et al. [3] give the total internal partition sums for ozone at 296K as 3473, 7385 and 3599 for isotopomers $^{16}O_3$, $^{16}O^{16}O^{18}O$ and $^{16}O^{18}O^{16}O$ respectively. These compare well with our values of 3483.71, 7465.67 and 3647.08.

N_2O

Five species of N_2O were considered in this study: $^{14}N_2{}^{16}O$, $^{14}N^{15}N^{16}O$, $^{15}N^{14}N^{16}O$, $^{14}N_2{}^{18}O$ and $^{14}N_2{}^{17}O$. Rotational energy levels were derived using the constants of Toth [27]. Because of its symmetry, there are no state dependent degeneracy factors for any N_2O species. The state independent factors used were 9, 6, 6, 9 and 54 for the species $^{14}N_2{}^{16}O$, $^{14}N^{15}N^{16}O$, $^{15}N^{14}N^{16}O$, $^{14}N_2{}^{18}O$ and $^{14}N_2{}^{17}O$, respectively. The direct sum, Q_{rot}, converged up to about 450K for the principal species.

The analytical expression used for Q_{rot} was that of McDowell [5]. The constants used for the analytical expression were those of Ref. [27]. The greatest difference exhibited between the converged direct sum and the analytical expression within the temperature range of interest was about 6.0 %. The analytical expression was used for the entire temperature range for all species.

The vibrational fundamentals used to calculate the vibrational partition sum were those of Ref. [14] and are presented in Table 5.

The partition sum calculated for N_2O agrees well with the value reported by Young [28], Q_{rot}=564.1 at 300K neglecting the state independent factor of 9 for this species, compared with our value for the rotational partition sum of 4497.37 for the principal species.

CO

Six species of CO were considered in this study: $^{12}C^{16}O$, $^{13}C^{16}O$, $^{12}C^{18}O$, $^{12}C^{17}O$, $^{13}C^{18}O$ and $^{13}C^{17}O$. Energy levels were derived using the Dunham constants of Guelachvili et al. [29] and the Y_{oo} constants of Tipping [30]. There are no state dependent degeneracy factors for any of these species. The state independent degeneracy factors are 1, 2, 1, 6, 2 and 12 for species $^{12}C^{16}O$, $^{13}C^{16}O$, $^{12}C^{18}O$, $^{12}C^{17}O$, $^{13}C^{18}O$ and $^{13}C^{17}O$, respectively. Q_{rot} by direct sum converged up to about 1400 K, 1300 K, 1300 K, 1300 K and 1300 K for species $^{12}C^{16}O$, $^{13}C^{16}O$, $^{12}C^{18}O$, $^{12}C^{17}O$ and $^{13}C^{18}O$ respectively.

The analytical expression of Q_{rot} was that of McDowell [5]. The rotational constants used for the analytical expression were those of Ref. [29]. The greatest differences exhibited between the direct sum and the analytical expression for points at which the direct sum remained converged in the temperature range of interest were approximately 10% for all species. However, the differences between the two methods of calculation remained under 1% until over 600K. The analytical expression was used throughout the entire temperature range for all species.

The vibrational partition sum was calculated using the vibrational fundamentals of Ref. [29] and are reported in Table 6.

The values calculated for the partition sums of CO in this study compare favorably with other published values. For example, the value of the rotational partition sum of the principal species at 300K from this study is 107.12, as compared to the value of 108.78 from Ref. 15.

CH_4

Three species of methane were considered in this study: $^{12}CH_4$, $^{13}CH_4$ and $^{12}CH_3D$. For all three of these species, the rotational partition sums were calculated using analytical formulae. Specifically, McDowell's formula for symmetric top molecules [9] was used for the deuterated species, while McDowell's formula for spherical top molecules [8] was used for the other two species. The constants used were those of Tarrago et al. [31] for species $^{12}CH_4$, Dang-Nhu et al. [32] for species $^{13}CH_4$ and Tarrago et al. [33] for $^{12}CH_3D$.

For $^{12}CH_4$ and $^{13}CH_4$ the state dependent degeneracy factors are 5, 3, and 2 for A, F, and E levels. For $^{12}CH_3$ D the state dependent degeneracy factors are 2 and 1 for the A and E levels [10]. However in the analytical calculations the symmetry number is used, which is 4/3, 4/3, and 8/3 for $^{12}CH_4$, $^{13}CH_4$, and $^{12}CH_3$ D, respectively.

Vibrational partition sums for all isotopomers were calculated using the vibrational fundamentals of the principal isotopomer taken from Norton and Rinsland [34], ν_1=2917 cm^{-1}, ν_2 (doubly degenerate)=1533 cm^{-1},ν_3 (3-fold degenerate)=3019 cm^{-1}, and ν_4 (3-fold degenerate)=1311 cm^{-1}.

The rotational partition sums determined here can be compared with other published values. For example, the Q_r(300K) values from this study are 598.65, 1197.22 and 4841.36 for the $^{12}CH_4$, $^{13}CH_4$ and $^{12}CH_3D$ species, respectively. These may be compared with the values of Robiette and Dang-Nhu [35] of 598.6, 598.6 and 1613.8, bearing in mind that their values neglect the state independent factors of 1, 2, and 3 for $^{12}CH_4$, $^{13}CH_4$ and $^{12}CH_3D$ species, respectively.

O_2

Three species of molecular oxygen were considered in this study: $^{16}O_2$, $^{16}O^{18}O$ and $^{16}O^{17}O$. Oxygen is a difficult molecule to model analytically because it has low-lying electronic states. Specifically, the ground state of O_2 is an $X^3\Sigma_g^-$ state, while the molecule also exhibits an $a^1\Delta_g$ state at approximately 7892 cm^{-1} and a $b^1\Sigma_g^+$ state at about 13130 cm^{-1}. These excited states must be included in a proper calculation of Q(T). For all species of oxygen considered in this study, direct sums were used throughout the entire temperature range. Assuming that the total energy of any given state is completely separable into its electronic, vibrational and rotational parts, the total internal partition function is determined by a product approximation formula Eq. 3:

Rotational energy levels were calculated for the ground vibrational state of each electronic state using the constants of Ref 36. Different vibrational constants were used for each electronic state from Ref 36. Once a complete set of ro-vibrational energy levels was calculated for each electronic state, a direct sum was calculated over this complete set of energies. Convergence tests indicated that these direct sums remained converged throughout the entire temperature range of interest.

The state independent statistical factors are 1, 1 and 6 for species: $^{16}O_2$, $^{16}O^{18}O$ and $^{16}O^{17}O$ respectively. For a complete description of the state dependent factors see Refs. 36, 37. In the electronic ground state of $^{16}O_2$, the only allowed rotational wave functions are those for odd (antisymmetric) N. In the $a^1\Delta_g$ electronic state, the resultant of the individual electron spin is zero (S=0) giving J=N, but the rotational levels are split into two, one symmetric (+) and one antisymmetric (-) state, by Λ-doubling. Because of the constraints placed on the wavefunction by Bose-Einstein statistics, only the (+) state

is allowed and, although all N are occupied, only half the states are realized. The $b^1\Sigma^+_g$ electronic state also has S=0 giving N=J, and the electronic wavefunction for the Σ^+_g state is symmetric as are Ψ_{nuc} and Ψ_{vib}. Thus the only rotational wavefunctions are the symmetric (N even) ones. Because of the symmetry of the $^{16}O_2$ species and the nuclear spin I(^{16}O)=0, half of the rotational states of *each* electronic level are missing.

For the two isotopic species on the database, $^{16}O^{18}O$ and $^{16}O^{17}O$, inversion through the center is no longer a valid symmetry operation. For this condition, all rotational levels of the molecule are allowed, both (+) and (-).

Values of the partition sum calculated in this study agree quite well with other published values. For the principal species, our values at 294K and 300K are 214.31 and 218.69, respectively. These compare favorably with the values of 213.9 and 218.655 from Refs. 38 and 15, respectively. A recent study by Schermaul [39] reported that the total internal partition sum for $^{16}O^{18}O$ at 296K was 455.9, while our value was 452.31.

NO

Three species of NO were considered in this study: $^{14}N^{16}O$, $^{15}N^{16}O$ and $^{14}N^{18}O$. Rotational energy levels were derived using the constants of Amiot et al. [40] and Meerts [41] for the $\Pi_{1/2}$ e, $\Pi_{1/2}$ f, $\Pi_{3/2}$ e and $\Pi_{3/2}$ f states. Direct rotational sums were calculated using these energies. There are no state dependent degeneracy factors for these species. The state independent factors are 3, 2 and 3 for species $^{14}N^{16}O$, $^{15}N^{16}O$ and $^{14}N^{18}O$ respectively. Convergence tests indicated that the direct sums remained converged up to about 2000 K, 800 K and 1000 K for species $^{14}N^{16}O$, $^{15}N^{16}O$ and $^{14}N^{18}O$ respectively.

The analytical expression of Q_{rot} used for NO was that of McDowell [5], with the same constants given above. The rotational partition sum can be expressed as a sum over all energies of the $\Pi_{1/2}$ and $\Pi_{3/2}$ states:

$$Q_r = \sum_{all\ states\ ,\ i} g_i e^{-hcE_i / kT}$$
$$= \sum_{all\ \Pi_{1/2}\ states} g_i e^{-hcE_i / kT} + \sum_{all\ \Pi_{3/2}\ states} g_i e^{-hcE_i / kT} \qquad (7)$$

Since the energies of the $\Pi_{1/2}$ and $\Pi_{3/2}$ states are separated by a roughly constant value, δE, of about 118 wavenumbers, the analytical partition sum can be written as

$$Q_r = \sum_{all\ \Pi_{1/2}\ states} g_i e^{-hcE_i / kT} \left(1 + e^{-hc\,\delta E / kT}\right)$$
$$= Q_{rot_{analytical}} \left(1 + e^{-hc\,\delta E / kT}\right) \qquad (8)$$

where Q_r(analytical) is calculated using the formalism of McDowell.

Comparisons between the direct sum and the analytical expression of Q_{rot} showed that the greatest differences at temperatures within the range of interest where the direct sum remained converged were 1.23% at approximately 118K for species 46 and 48 and about 0.75% at 75K for species 56. However, these differences dropped to about 0.3%

for all species by 750K. For all species, an analytical expression was used throughout the temperature range.

The vibrational partition sum for this species was calculated using the vibrational fundamentals of Ref. 2, 1876.0765 cm^{-1}, 1843.020 92 cm^{-1}, 1827.387 16 cm^{-1}, for the $^{14}N^{16}O$, $^{15}N^{16}O$, and $^{14}N^{18}O$ isotopomers, respectively. The corrections discussed in Ref. 3 were implemented in calculating the partition sums for this molecule. Since the hyperfine splitting for this species is directly accounted for in the direct sum and handled approximately in the analytical expression, it is inappropriate to include the product of the spins of the nuclei as a state independent factor. With these corrections, our value of the partition sum for the principal species of NO, 1142.13, agrees very well with the value from Goldman et al. [3], 1140.93.

SO_2

Two species of SO_2 are considered in this study: $^{32}S^{16}O_2$ and $^{34}S^{16}O_2$. Rotational energy levels were calculated using the constants of Pine et al. [42]. Tests indicated that the direct sum of Q_{rot} remained converged up to approximately 250K. The state independent statistical factors are 1 for both species. The state dependent factors are 0-fold for odd states and 1-fold for even states (i.e. odd states do not exist).

The analytical formula used for Q_{rot} was that of Watson [6]. The molecular constants used were those of Ref. 42. A comparison of the direct sum with the analytical expression revealed that the greatest difference between the two methods at points in the temperature range of interest where the direct sum remained converged was about 0.12%,

which occurred at 75K. At 250K, the difference was about 0.006%. The analytical expression was used throughout the temperature range of interest for both species.

Vibrational partition sums were calculated for both species using the vibrational constants of Lafferty et al. [43], which are 1151.71 cm^{-1}, 517.89 cm^{-1}, and 1362 cm^{-1} for the ν_1, ν_2, and ν_3 fundamentals of $^{32}S^{16}O_2$ and 1152 cm^{-1}, 518 cm^{-1}, and 1362 $cm^{-1}$for the ν_1, ν_2, and ν_3 fundamentals of $^{34}S^{16}O_2$.

Partition sums calculated for SO_2 in this study agree quite well with other published values. For example, recent spectroscopic studies by Lafferty et al. [43, 44] and by Chu et al. [45], both give the total internal partition sum for the $^{32}S^{16}O_2$ species at 296K as 6345, which compares favorably with our value of 6340.29.

NO_2

One species of NO_2 was considered in this study: $^{14}N^{16}O_2$. Rotational energy levels for direct summation were produced using the formalism of Perrin et al. [46], which includes electron spin-rotation and hyperfine Fermi resonances. The state independent degeneracy factor is 3. The state dependent factors are 0-fold for odd states and 1-fold for even states (i.e. odd states do not exist). Tests indicated that Q_{rot} converged up to approximately 150K.

Watson's analytical expression of Q_{rot} [6] was used. Molecular constants for the expression were taken from Perrin et al. [46]. A comparison of the direct sum with the analytical expression revealed that the greatest difference between the two methods at points within the temperature region of interest for which the direct sum remained

converged was about 0.37%. The analytical expression was used throughout the temperature range.

The vibrational partition function was calculated using the vibrational fundamental reported by Norton and Rinsland [34]; 1320 cm^{-1}, 750 cm^{-1}, and 1617 cm^{-1} for the ν_1, ν_2, and, ν_3 fundamentals.

The total internal partition sum determined in this work at 296K, 13 577.48, compares well with that given in Ref. 46, 13 617.9.

NH_3

Two isotopomers of ammonia were considered in this study: $^{14}NH_3$ and $^{15}NH_3$. Energy levels for direct summation to produce Q_{rot} were created using the constants of Poynter and Margolis [47] for the $^{14}NH_3$ species and Carlotti et al. [48] for the $^{15}NH_3$ species. The direct sum remained converged up to approximately 1800 K for the $^{14}NH_3$ species and 1600 K for the $^{15}NH_3$ species. The state-independent statistical factors used were 3 and 2 for species $^{14}NH_3$ and $^{15}NH_3$, respectively. The state-dependent factor is 4 for states with K=0 or K equal to a multiple of 3, and is 2 for all other states.

The analytical expression of Q_{rot} used for ammonia was that of McDowell [9], with the constants from the references cited above. A comparison of the direct sum with the analytical expression in the converged region revealed that the greatest difference between the two methods for the $^{14}NH_3$ species was 0.78% at 75K. However, at 1800K, the difference between the two methods was about 0.13%. For the $^{15}NH_3$ species, the

maximum difference was only about 0.15%. The analytical expression was used for both species throughout the entire temperature range.

The vibrational partition function for $^{14}NH_3$ was calculated using the vibrational constants from Norton and Rinsland [34], ν_1=3337 cm^{-1}, ν_2=950 cm^{-1}, ν_3 (2-fold degenerate)=3444 cm^{-1}, and ν_4 (2-fold degenerate)=1630 cm^{-1}. For $^{15}NH_3$ the vibrational partition function used the values for $^{14}NH_3$.

The partition functions calculated for ammonia in this study agree well with other published data. For the $^{14}NH_3$ species, an accurate expression for the partition sum of NH_3 was derived by Urban et al. [49] and yielded a value of 1731.48 for the total internal partition sum at 296K, which compares favorably with our value of 1725.22. Similarly, values of 569.231 and 568.27 were reported by Pine and Dang-Nhu [50] and Aroui [51], respectively. These values neglect the state independent factor arising from the spin of the nitrogen atom, so they are a factor of three smaller than the values from this study. For the $^{15}NH_3$ species, our value of 1152.65 compares quite well with the values of Devi et al. [52] and the JPL Catalog [15], scaled to 296K, which are 1153.31 and 575.837. Note that the JPL value is too small by a factor of two due to neglecting the state independent factor from the spin of the nitrogen atom and it also omits Q_{vib}, which is 1.0107 at 296 K.

HNO_3

One species of nitric acid is considered in this study: $H^{14}N^{16}O_3$. The rotational partition function was evaluated at all temperatures using the analytical expression of

Watson [6] and the rotational constants of Maki and Wells [53]. The state independent statistical factor was 6. There are no state dependent statistical factors for this species.

The vibrational partition sum was calculated using the vibrational constants from Norton and Rinsland [34] and are given in Table 7.

Our value of the total internal partition sum at 300K is 214 126.7, which is consistent with the value reported by Maki [54] of 27 343 (*Qrot*) x 1.304 (*Qvib*) x 6 ([*2I(H)+1*] x [*2I(N)+1*]) = 213 931.6.

OH

Three species of the hydroxyl radical were considered in this study: ^{16}OH, ^{18}OH and ^{16}OD. Rotational energy levels were produced using the method of Beaudet and Poynter [55], which includes fine structure interaction and lambda doubling. These energies were calculated for the $\Pi_{1/2}$, $\Pi_{3/2}$ and $\Sigma_{1/2}$ states. Tests indicated that the direct sum remained converged throughout the entire temperature range of interest. The state independent degeneracy factors are 2, 2 and 3 for species ^{16}OH, ^{18}OH, and ^{16}OD respectively. There are no state dependent factors for any of these species. The direct sum was used for Q_{rot} for all of these species throughout the entire temperature range of interest.

Vibrational partition sums were calculated using the vibrational constants of Ref. 55; 3569.643 cm^{-1} for ^{16}OH, 2632.13 cm^{-1} for ^{18}OH and ^{16}OD used the principal isotopologue value. The corrections discussed in Goldman et al. [3] were implemented in calculating the partition sums for this species. Since the fine structure of the molecule is

modeled directly in the rotational direct sum, the product of the spins of the nuclei must not be included as a state independent factor. The partition sums from this study compare favorably with those of Ref. 3. For example, for the principal species of OH at 296K, we obtained 80.3622, which is quite similar to the value 80.3469 given in Ref. 3.

Hydrogen Halides

Six species of hydrogen halides are considered in this study: $H^{19}F$, $H^{35}Cl$, $H^{37}Cl$, $H^{79}Br$ and $H^{81}Br$ and $H^{127}I$. The ro-vibrational energy states of these species are calculated using the Dunham formulation and the molecular constants of Refs. 56-59. For all species, the direct sum over these ro-vibrational energy levels remained converged throughout the temperature range of interest and was used for all species at all temperatures. The state independent statistical factors are 4, 8, 8, 8, 8 and 12 for $H^{19}F$, $H^{35}Cl$, $H^{37}Cl$, $H^{79}Br$ and $H^{81}Br$ and $H^{127}I$. There are no state dependent statistical factors for any of these species. Neither the product approximation nor the harmonic oscillator approximation was used for any of these species.

The values of the partition sums obtained in this study agree well with other published values. For $H^{35}Cl$ and $H^{37}Cl$, we obtained 162.80 and 163.04 at 300K, respectively. These are similar to the JPL [15] values of 81.232 and 81.352, which include the spin of the chlorine but neglect the spin of the hydrogen atom, and therefore are too small by a factor of 2. For $H^{79}Br$ and $H^{81}Br$, at 300K we obtained 202.85 and 202.91, respectively, which are similar to the JPL values of 101.2045 and 101.2511 respectively, considering that these values also omit the spin of the hydrogen atom. Note,

the comparison is made to the JPL Q_{rot} values since Q_{vib}(300 K) = 1.0000 for these isotopomers.

ClO

Two species of ClO were considered in this study: $^{35}Cl^{16}O$ and $^{37}Cl^{16}O$. The rotational energies of these species were calculated using the formalism of Endo et al. [60] and using the constants of Cohen et al. [61] The energies of the $\Pi_{1/2}$ and $\Pi_{3/2}$ states were calculated, producing a set of energies complete to about 9500 wavenumbers. Tests indicated that for both species, the direct sum for Q_{rot} remained converged up to about 500K. The state independent factor due to nuclear spin is 4 for both species. However, these are not used since the hyperfine structure is explicitly considered. There are no state dependent degeneracy factors for both species.

The analytical expression of Q_{rot} used for ClO was that of McDowell [5]. ClO was analytically modeled in much the same way as NO. The energies of the $\Pi_{3/2}$ states were accounted for by the addition of another term which multiplies the partition function since the separation between the $\Pi_{1/2}$ and the $\Pi_{3/2}$ states is roughly a constant at about 321.55 wavenumbers. Additionally, a statistical factor of 2 was added to account for e/f splitting and a factor of 4 was added to account for hyperfine F states. A comparison of the direct sum with the analytical expression revealed that the greatest difference between the two methods at points where the direct sum remained converged in the temperature range of interest was about 2.41% for the $^{35}Cl^{16}O$ species and 2.37% for the $^{37}Cl^{16}O$ species. Both of these values occurred at 70K. However, by 500K, the difference

between the two methods was only about 0.064% for the $^{35}Cl^{16}O$ species and .053% for the $^{37}Cl^{16}O$ species. For both species, the direct sum was used for temperatures up to and including 500K, while the analytical expression was used for all temperatures greater that 500K.

The vibrational partition sum was calculated using the vibrational fundamentals of 841.6 cm^{-1} and 837.2 cm^{-1} for $^{35}Cl^{16}O$ and $^{37}Cl^{16}O$ isotopomers [34]. The corrections discussed in Ref. 3 were utilized in calculating the partition sums for this molecule. As the hyperfine splitting is handled explicitly in the direct sum and approximately in the analytical expression, it is inappropriate to use the product of the spins of the nuclei as a state independent factor. With these corrections, our value of the partition sum for $^{35}Cl^{16}O$ at 296K is 3291.30, which compares favorably with the value of 3227.77, given in Goldman et al. [3].

OCS

Five isotopomers of OCS were considered in this study: $^{16}O^{12}C^{32}S$, $^{16}O^{12}C^{34}S$, $^{16}O^{13}C^{32}C$, $^{18}O^{12}C^{32}S$ and $^{16}O^{12}C^{33}S$. The rotational energies for direct summation of Q_{rot} were calculated using the constants of Maki [62]. Energies were calculated for all species except $^{16}O^{12}C^{33}S$. Tests indicated that the direct sum remained converged up to approximately 450K for all of these species. The state independent degeneracy factors are 1, 1, 2, 1 and 4 for $^{16}O^{12}C^{32}S$, $^{16}O^{12}C^{34}S$, $^{16}O^{13}C^{32}C$, $^{18}O^{12}C^{32}S$ and $^{16}O^{12}C^{33}S$ respectively. There are no state dependent degeneracy factors for any of these species.

The analytical expression for Q_{rot} of OCS was that of McDowell [5], with the constants of Maki [62]. A comparison of the direct sum with the analytical expression revealed that the greatest differences at points where the direct sum remained converged within the temperature range of interest were about 0.45% for all species. The analytical expression was used for all species at all temperatures.

The vibrational partition sums were calculated using the vibrational fundamentals as follows: for ν_3 for all isotopomers the data are from Hunt et al. [63]; for the $^{16}O^{12}C^{32}S$ isotopomer ν_1 is from Wells et al. [64] and ν_2 is from Mürtz et al. [65]; ν_1 of the $^{16}O^{12}C^{34}S$ isotopomer is from Tan et al. [66], ν_2 of this isotopomer and ν_1 and ν_2 of the $^{16}O^{13}C^{32}S$ and $^{16}O^{12}C^{33}S$ isotopomers are from Brown and Fayt [67]; and ν_1 and ν_2 of the $^{18}O^{12}C^{33}S$ isotopomer are estimated from the principal isotopomer by isotopic mass scaling using the ν_3 values. The values are presented in Table 8.

The partition sums calculated for OCS in this study compare favorably with other published values. Bouanich et al. [68] reported a value of 1229.21 at 298K for the $^{16}O^{12}C^{32}S$ species, while our value is 1233.49. Blanquet et al. [69] give values of the rotational partition sum at 298K as 1047.4, 1025.1 and 1034.8 for the $^{16}O^{12}C^{34}S$, $^{16}O^{13}C^{32}S$ and $^{16}O^{12}C^{33}S$ species respectively, which compare well with our values of 1050.72, 2056.68 and 4152.39, once the state independent factors are properly accounted for in their partition sums.

H_2CO

Three species of formaldehyde are considered in this study: $H_2{}^{12}C^{16}O$, $H_2{}^{13}C^{16}O$ and $H_2{}^{12}C^{18}O$. Rotational energies for the first two species were calculated using the constants of Winnewisser et al. [70]; for $H_2{}^{12}C^{18}O$ the constants of Dangoisse et al. [71] were used. Tests indicated that the direct sums of Q_{rot} remained converged up to approximately 1000K for the species. The state independent statistical factors are 1, 2 and 1 for $H_2{}^{12}C^{16}O$, $H_2{}^{13}C^{16}O$ and $H_2{}^{12}C^{18}O$ species respectively. The state dependent degeneracy factors are 3 for odd rotational states and 1 for even rotational states.

Watson's analytical expression of Q_{rot} was used [6]. This expression was implemented for all three species on the HITRAN database. A comparison of the direct sum with the analytical expression for the two species for which it was available revealed that the greatest difference between the two methods was about 11.8%. The analytical expression was used for all three species at all temperatures.

The vibrational partition sums were calculated for $H_2{}^{12}C^{16}O$ using the vibrational constants from Norton and Rinsland [34]; ν_1=2782 cm^{-1}, ν_2=1746 cm^{-1}, ν_3=1500 cm^{-1}, ν_4=1167 cm^{-1}, ν_5=2843 cm^{-1}, and ν_6=1249 cm^{-1}. For $H_2{}^{13}C^{16}O$, Q_{vib} was that of the principal species.

The values calculated for the rotational partition sums at 300K in this study of 2885.39 and 5916.98 for the $H_2{}^{12}C^{16}O$ and $H_2{}^{13}C^{16}O$ isotopomers, respectively agree well with the values given in Ref. 15 of 2876.7 and 2949.7, considering that the value for the $H_2{}^{13}C^{16}O$ species omits the state independent factor of 2 coming from the spin of the carbon atom.

HOCl

Two isotopomers of HOCl were considered in this study: $H^{16}O^{35}Cl$ and $H^{16}O^{37}Cl$. Rotational energy levels were calculated using the constants of Lovas [72]. Tests indicated that the direct sum rotational partition functions remained converged up to about 250K for the $H^{16}O^{35}Cl$ species and 200K for the $H^{16}O^{37}Cl$ species. The state independent statistical factor is 8 for both species. There are no state dependent statistical factors for HOCl.

The analytical expression of Q_{rot} used for HOCl was that of Watson [6], with the same rotational constants used for the direct sum. A comparison of the two methods indicated that the greatest differences which occurred at points in the temperature range of interest where the direct sum remained converged were 0.061% and 0.051% for species $H^{16}O^{35}Cl$ and $H^{16}O^{37}Cl$ respectively. The analytical expression was used for both species at all temperatures.

The vibrational partition sums for both isotopomers were calculated using the vibrational fundamentals reported by Norton and Rinsland [34]; ν_1=3069 cm^{-1}, ν_2=1239 cm^{-1}, and ν_3=724.0 cm^{-1}.

The values of the rotational partition sum calculated in this study agree well with other published data. Our values at 300K are 19 700.13 and 20 049.08 for the $H^{16}O^{35}Cl$ and $H^{16}O^{37}Cl$ species respectively. Once the state independent factor of 8 for both species is considered, these values agree well with the JPL values [15] of 2380 and 2422.5.

N_2

Only the principal species of N_2 was considered in this study. Rotational energies were calculated using the Dunham coefficients of Reuter et al. [73]. The resulting energy levels were complete to about 11 000 wavenumbers and extend as high as 31 000 wavenumbers. Tests indicated that the direct sum of Q_{rot} remained converged up to approximately 2000 K. For N_2, the state independent factor is 1, while the state dependent statistical factors are 6-fold for the even states and 3-fold for the odd states.

The analytical expression of Q_{rot} used for this species was McDowell's [5]. An average spin factor of 4.5 was used to account for the different weights of the even and odd states. A comparison of the direct sum with the analytical expression revealed that the greatest difference between the two methods at points where the direct sum remained converged was about 0.56%. The analytical expression was used throughout the entire temperature range.

The vibrational partition function was calculated taking the vibrational fundamentals of N_2 as 2329.912 39 cm^{-1} [73].

The rotational partition sum obtained in this study, 469.12 at 298 K, compares well with Ref. 73, 469.7.

HCN

Three species of HCN were considered in this study: $H^{12}C^{14}N$, $H^{13}C^{14}N$ and $H^{12}C^{15}N$. A complete set of rotational energies to about 8,000 wavenumbers were calculated using the constants of Maki [62]. Tests revealed that the direct sum over

rotational energies remained converged up to about 500 K for all species. The state independent statistical factors are 6, 12 and 4 for species $H^{12}C^{14}N$, $H^{13}C^{14}N$ and $H^{12}C^{15}N$, respectively. There are no state dependent statistical factors for all species of HCN.

The analytical expression of McDowell [5] was used for Q_{rot} with the rotational constants of Maki. A comparison of the direct sum and the analytical expression revealed that the greatest difference between the two methods at points for which the direct sum remained converged was about 1.32% for the $H^{12}C^{15}N$ species and about 0.50% for the other two species. The analytical expression was used for all species at all temperatures.

The vibrational partition sum was calculated using the vibrational fundamentals from Norton and Rinsland [34] and are reported in Table 9.

Comparing our values at 300K with other data we find the JPL catalog [15] gives values of 424.326, 435.412 and 145.680 for the rotational partition sums of species $H^{12}C^{14}N$, $H^{13}C^{14}N$ and $H^{12}C^{15}N$ respectively, while our values are 851.50, 1748.11 and 589.44. Note, the JPL values only include the state independent factors due to the spin of ^{14}N for the first two isotopomers, thus their values are lower than ours by factors of 2, 4, and 4. For the principal species McDowell [5] reports a value of Q_{rot}=141.4662 at 300 K compared to our value of 851.5047 which includes the state independent factor of 6.

CH_3Cl

Two species of CH_3Cl were considered in this study: $^{12}CH_3{}^{35}Cl$ and $^{12}CH_3{}^{37}Cl$. The rotational partition function was calculated using McDowell's analytical expression

[9] with the constants of Di Lauro and Alamichel [74]. The state dependent statistical factors are 4 for states with K equal zero or a multiple of 3 and 2 for other states. While hyperfine structure due to chlorine and *l*-type doubling are known for CH_3Cl, HITRAN includes only vibrational-rotational lines. The state independent factors for both species, d_i=8, includes the hyperfine structure due to chlorine (4) and the *l*-type doubling (2). Including the hyperfine structure implies that g_i=1.

The vibrational partition functions for both species were calculated using the vibrational constants of the $^{12}CH_3{}^{35}Cl$ species taken from Norton and Rinsland [34]; ν_1=2968 cm^{-1}, ν_2=1355 cm^{-1}, ν_3=733 cm^{-1}, ν_4 (2-fold degenerate)=3039 cm^{-1}, ν_5 (2-fold degenerate)=1452 cm^{-1}, ν_6 (2-fold degenerate)=1018 cm^{-1}.

Blanquet et al. [75, 76] report direct sum calculations for $^{12}CH_3{}^{35}Cl$ and $^{12}CH_3{}^{37}Cl$. They list Q_{rot}(297K)=13 896 and Q_{rot}(296K)=14 050; Q_{vib}(296K)=1.0479 and Q_{vib}(296K)=1.0473; which yields Q_{tot}(297K)=14 561.6 and Q_{tot}(296K)=14 714.6 for the two isotopomers, hence hyperfine and *l*-type doubling are omitted. Dang-Nhu et al. [77] report the same Q_{vib} and give Q_{tot}(296K)=4 x 14 492 for the $^{12}CH_3{}^{35}Cl$ species (hyperfine included). These values compare well with the values calculated in this work, Q_{tot}(296K)=8 x 14 562 and Q_{tot}(296K)=8 x 14 479 for the $^{12}CH_3{}^{35}Cl$ and $^{12}CH_3{}^{37}Cl$ isotopomers, respectively.

H_2O_2

There are a number of complications to the determination of the partition sums for H_2O_2. The molecule has a number of torsional states that must be accounted for in the

sum. There are not enough energy levels available to calculate the partition sums over the desired temperature range. Tests made using available energy levels in a direct sum of $Q_{rot\text{-}tors}$ show convergence up to about 500 K. Finally, the analytical model presented below was developed using a number of approximations. Hence, the partition sums at high temperatures may be questioned. For a discussion of the complexity of this system see Goldman et al. [3].

The energy structure includes tunneling through the (low, ~390 cm^{-1}) *trans* barrier (C_{2h} form) and the (high, ~2560 cm^{-1}) *cis* (C_{2v} form) barrier. For the *trans* tunneling the number of rotational levels is doubled, i.e. (J, K_a, K_c) for both τ=1,2 and τ =3,4. For the *cis* tunneling, the levels are restricted to (J, K_a =even, K_c) for the τ =1, 4 and to (J, K_a =odd, K_c) for the τ =2, 3. It might appear at first that a simple doubling of the rotational levels by the tunneling through the low trans barrier would give a useful approximation to the partition function. This is not sufficient because the tunneling induces a splitting which increases from ~11 cm^{-1} (for n=0) to ~106.3 cm^{-1} (n=1), to ~206 cm^{-1} (n=2) etc. and the rotational constants (A, B, C, Δ_K, etc.) vary significantly from one torsional state to another.

As pointed out by Goldman et al. [3] the torsional-rotational partition sum for H_2O_2 can be written

$$Q_{tors-rot} = \sum_{\tau=1}^{4} \sum_{n=0}^{\infty} \sum_{J,K_a,K_c} (2J+1)\, d_{\tau JK_aK_c} \exp\left(-\frac{E_{n\tau JK_aK_c}}{kT}\right) \qquad (9)$$

where τ designates the sublevels of the torsional state *n* (with torsional dependence of the rotational constants) and $d_{\tau,J,Ka,Kc}$ are nuclear spin statistical weights, which arise due to the exchange of the two hydrogen atoms and of the two oxygen atoms. For H_2O_2 one finds that the A_{gs} and A_{us} (B_{gs} and B_{us}) vibration torsion rotation wavefunctions exist with a nuclear weight of 1 (3). The state independent statistical factor is 1 for H_2O_2. This expression can be related to an analytical expression, which assumes a complete set of states from $J=K_a=K_c=0$ to infinity, by considering the energy structure for the torsional states. The τ=1 and τ=4 levels have K_a even and the τ=2 and τ=3 levels have K_a odd. Thus τ=1 and τ=2 taken together comprise a complete set of states as does τ=3 and τ=4. Thus in a shorthand notation Eq. 9 can be written

$$Q_{tors-rot} = \sum_{\substack{J,Ka,Kc,\\ n=0\ to\ \infty,\\ \tau=1,2}} g_s \exp\left(-\frac{E_s}{kT}\right) + \sum_{\substack{J,Ka,Kc,\\ n=0\ to\ \infty,\\ \tau=3,4}} g_s \exp\left(-\frac{E_s}{kT}\right) \qquad (10)$$

where g_s, given by d_s $(2J+1)$, is the statistical degeneracy factor and E_s the energy of state *s*. Working with the first term, the sublevel τ = 1 starts at $J=Ka=Kc=0$ with energy equal to zero. The sub level τ=2 completes the set of rotational states. For a given rotational state, *J*, K_a, K_c, the torsional states can be grouped, here for the τ = 1 state,

$$g_{(\tau_1 J K_a K_c)} e^{-E_{n=0}/kT} + g_{(\tau_1 J K_a K_c)} e^{-E_{n=1}/kT} + g_{(\tau_1 J K_a K_c)} e^{-E_{n=2}/kT} + \bullet\bullet\bullet$$

where *n* goes to infinity.

Using the potential surface for H_2O_2 [78], the energies of the different *n* states for each torsional state can be determined. These are given in Table 10 for n up to 7. For all the higher (*n*>=2) τ=1,2 or τ =3,4 torsional states the value is different because of the staggering effect. The energy of a state $E(n, \tau)[J,Ka,Kc]$ can be approximated by $E(n, \tau)_{calculated} + E(n=0, \tau=1)[J,Ka,Kc]$, where $E(n=0, \tau=1)[J,Ka,Kc]$ is the energy level for *n*=0 and τ =1. For a given state [*J,Ka,Kc*], a short hand notation is adopted; $E_{n=x}=E(x, \tau)$, $\Delta E_{n=x}= E(x, \tau)_{calculated}$, and $E_{n=0}= E(n=0, \tau=1)$ and the expression above can be rewritten,

$$g_{(\tau_1 J K_a K_c)} e^{-E_{n=0}/kT}\left[1 + e^{-\Delta E_{n=1}/kT} + e^{-\Delta E_{n=2}/kT} + e^{-\Delta E_{n=3}/kT} + \bullet\bullet\bullet\right]$$

Thus the first term of the partition sum would look like

$$\sum_{\substack{J,Ka,Kc,\\ n=0\ to\ \infty,\tau=1,2}} g_S \exp\left(-\frac{E_S}{kT}\right) = Q_{analytical}\left[1 + e^{-\Delta E_{n=1}/kT} + e^{-\Delta E_{n=2}/kT} + e^{-\Delta E_{n=3}/kT} + \bullet\bullet\bullet\right] \tag{11}$$

where $Q_{analytical}$ is an analytical form for the rotational partition function for an asymmetric rotor. This can be approximated by the formula of Watson [6]. The sum in the square brackets can be taken to $\Delta E_{n=7}$, where the values for the $\Delta E_{n=x}$ terms are taken from the last column of Table 10 neglecting the staggering effect.

For the second term of Eq. 9 the situation is more complicated because the energy of the lowest state (J=K_a=K_c=0, τ = 4) is at 11.437 438 cm^{-1}. The problem is that the analytical formulae rely on a full set of states starting at E=0. To correct for this the energy is scaled by the value E_{sc}=11.437 438. E_{sc} is added and subtracted from the energy of all of the τ =3,4 states. The partition sum for the second term can then be written

$$Q_{\tau=3,4} = e^{-E_{sc}/kT} \sum_{\substack{all\ states \\ \tau=3,4}} g_s e^{-E'_s/kT} \qquad (12)$$

where $E'_s = E_s - E_{sc}$. Realizing as before that for each particular rotational state there are energies for the torsional states, n, and defining the differences between the $E'_{n=0}$ state and the n=1 to 7 states as $\Delta E'_{n=1}$, $\Delta E'_{n=2}$, etc., the partition sum for the second term can be written

$$Q_{\tau=3,4} = Q_{analytical}\left[1 + e^{-\Delta E'_{n=1}/kT} + e^{-\Delta E'_{n=2}/kT} + e^{-\Delta E'_{n=3}/kT} + \bullet\bullet\bullet\right] e^{-E_{sc}/kT}$$

(13)

The analytical expression to determine the torsional-rotational partition function can now be written using Watson's analytical formula with the rotational constants for the $\tau = 1, 2$ and $\tau = 3, 4$ torsional states,

$$Q_{tors-rot} = Q_{Watson,\tau=1,2}\left[1 + e^{-\Delta E_{n=1}/kT} + e^{-\Delta E_{n=2}/kT} + e^{-\Delta E_{n=3}/kT} + \bullet\bullet\bullet\right] + Q_{Watson,\tau=3,4}\left[1 + e^{-\Delta E'_{n=1}/kT} + e^{-\Delta E'_{n=2}/kT} + e^{-\Delta E'_{n=3}/kT} + \bullet\bullet\bullet\right] e^{-E_{sc}/kT} \quad (14)$$

Vibrational partition sums were calculated using only the 5 "low amplitude modes, ν_1, ν_2, ν_3, (A_{gs} symmetry) and the ν_5, ν_6 (B_{us} symmetry), 3580. cm^{-1}, 1395.8 cm^{-1}, 865.939 37 cm^{-1}, 3780. cm^{-1}, and 1264.584 17 cm^{-1}, respectively, as suggested by the studies of Refs. 78, 79, 80, 81.

The direct sums converge up to about 500 K. Figure 4 shows the percent difference ($Q_{analytical}$-Q_{DS}) versus temperature, the top panel shows the percent difference from 50-600 K and the lower panel shows the percent difference for the temperature range of this work. The exact value of $Q(T)$ calculated by direct sum at 296K is 9851.664 73. The value calculated via Eq. 14 is 9819.750 19, 0.3% different.

C_2H_2

Two species of C_2H_2 were considered in this study: $^{12}C_2H_2$ and $^{12}C^{13}CH_2$. Rotational energies for both species were derived using the constants of Hietanen and

Kauppinen [82]. Tests indicated that the direct sum over the rotational energies remained converged up to approximately 1000 K for both species. The state independent statistical factors are 1 and 8 for the $^{12}CH_2$ and $^{12}C^{13}CH_2$ species respectively. The state dependent statistical factors for the $^{12}CH_2$ species are 1 for the even states and 3 for the odd states; for the $^{12}C^{13}CH_2$ species the state dependent factor is 1.

The analytical expression used for this molecule was that of McDowell [5], with the constants of Hietanen and Kauppinen [82]. A comparison of the direct sum with the analytical expression revealed that the greatest difference between the two methods was about 0.99% for both species. The analytical expression was used for both species at all temperature ranges.

The vibrational partition sums for both isotopomers were calculated using the principal isotopomer vibrational fundamentals of ν_1=3374, ν_2=1974, ν_3=3289, ν_4 (2)=612, and ν_5 (2)=730 [34].

The partition sums obtained for C_2H_2 compare well with published data. For example, our value of the rotational partition sum of $^{12}C_2H_2$ at 300K is 356.39, which is quite similar to the value from Ref. 5, 355.2551.

C_2H_6

Only the principal species of ethane was considered in this study. Rotational partition sums were calculated by McDowell's analytical expression [9], using the constants of Duncan et al. [83]. The state independent statistical factor for this species is

equal to 1. The symmetry number is given by 32/3. The analytical expression was used throughout the entire temperature range.

The vibrational partition sum was calculated using the vibrational fundamentals from Norton and Rinsland [34], but also including ν_4 = 303 cm^{-1}, which was omitted from Ref. 34, as discussed by Goldman et al. [3]. The values are presented in Table 11.

We can compare our value for the total internal partition sum at 50 K, 3590.781, with that of McDowell [9] who reports a value of Q_{rot} equal to 3595.181. At 300K we report a value of 72914.07 which can be compared with that of Pine and Rinsland [84], 76660.4. The comparison at 300 K demonstrates the need to add anharmonic corrections for torsion in ethane to our calculations. This is currently being pursued.

PH_3

Only the principal isotopic species of phosphine was considered in this study. A set of rotational energy levels complete to about 26 000 wavenumbers was calculated using the constants of Maki et al. [85]. Tests indicated that Q_{rot} remained converged throughout the temperature range of interest. The state independent statistical factor for this species is 2. The state dependent factor is 4 for states with K=0 or K equal to a multiple of 3 and is 2 for all other states. The direct sum for Q_{rot} was used for this species throughout the entire temperature range.

The vibrational partition function was calculated using the following vibrational constants with their uncertainty in parenthesis; ν_1 = 2321.1214(27) cm^{-1} [86], ν_2

=992.1301(23) cm^{-1}. [87], ν_3 (2-fold degenerate) = 2326.8766(23) cm^{-1} [86], and ν_4 (2-fold degenerate)=1118.3131(15) cm^{-1} [87].

The rotational partition sum calculated in this study was 3259.190 at 300K. This can be compared with the JPL [15] value of 803.896. After multiplying the JPL value by the state independent statistical factor of 2, their value is still a factor of 2 smaller than ours. Our value compares well with the classical rotational partition sum from Herzberg [10] of 1622.81 times 2 for the state independent factor $Q_{rot\text{-}class}$=3245.6

COF_2

Only the principal species of COF_2 was considered in this study. The rotational partition sum was calculated using the analytical formula of Watson [6] and the rotational constants of Goldman et al. [88]. The state independent statistical factor for this species is 1. The state dependent degeneracy factors are 3 for odd rotational states and 1 for even rotational states, hence a factor of 2 in the analytical formula. The analytical expression was used throughout the entire temperature range.

The vibrational partition sum was calculated using the vibrational fundamentals from Norton and Rinsland [34]; ν_1=1944 cm^{-1}, ν_2=963 cm^{-1}, ν_3=582 cm^{-1}, ν_4=1242 cm^{-1}, ν_5=619 cm^{-1}, and ν_6=774 cm^{-1}.

The partition sums for COF_2 compare favorably with other results from the literature. For example, the value of the rotational partition sum at 296K from this study is 60 476.27, while the value from Ref. 88 is 59 715.

SF_6

Only the principal isotopic species of SF_6 was considered in this study. The rotational partition sum was calculated using McDowell's analytical formula for spherical top molecules [8] using the rotational constants of Bobin et al. [89]. The state independent statistical factor is 1. The state dependent degeneracy factors are 2, 10, 8, 6, and 6 for the A_1, A_2, E, F_1 and F_2 levels, respectively. The averaged state dependent statistical factors needed in the analytical calculation is $\{(2*I_F+1)**6\}/24$. Given the spin of the fluorine nuclei, I_F = ½, this factor reduces to 8/3. The analytical expression was used throughout the entire temperature range.

The vibrational partition sum was calculated using the vibrational fundamentals; ν_1 (3-fold degenerate)=346 cm^{-1}, ν_2 (3-fold degenerate)=523 cm^{-1}, ν_3 (3-fold degenerate)=615 cm^{-1}, ν_4 (3-fold degenerate)=948 cm^{-1}, ν_5 (2-fold degenerate)=642 cm^{-1}, and ν_6=774 cm^{-1} [34].

The partition sums calculated in this study agree well with an approximate calculation made by Pine and Patterson [90] which gives the total internal partition sum at 160K as 2.423 x 10^5, which is quite close to our value of 2.42469 x 10^5. McDowell [8] reports a value of Q_{rot} at 5 K equal to 1121.216 which compares well with the value from this work, 1121.328.

H_2S

Three species of hydrogen sulfide were considered in this study: $H_2{}^{32}S$, $H_2{}^{34}S$ and $H_2{}^{33}S$. The rotational partition sums for all three species were calculated using Watson's analytical formula [6], with the rotational constants of Flaud et al. [91] The state independent degeneracy factors for H_2S are 1, 1 and 4 for the : $H_2{}^{32}S$, $H_2{}^{34}S$ and $H_2{}^{33}S$ species respectively. The state dependent degeneracy factors are 3 for odd rotational states and 1 for even rotational states. The analytical expression was used for all three species throughout the temperature range of interest.

The vibrational partition sums of all species were calculated using the vibrational fundamentals of the principal species ($H_2{}^{32}S$); ν_1=2615 cm^{-1}, ν_2=1183 cm^{-1}, and ν_3=2626 cm^{-1} [34].

The partition sums at 296K calculated in this study are 503.07, 504.35 and 2014.93 for the $H_2{}^{32}S$, $H_2{}^{34}S$ and $H_2{}^{33}S$ species, respectively. These can be compared with the values of 505.6, 506.9 and 506.2 from Ref. 91, considering that their value for the $H_2{}^{33}S$ species is too small by a factor of 4.

HCOOH

Only the principal isotopic species of formic acid was considered in this study. The rotational partition sum was calculated using Watson's analytical expression [6], with the rotational constants of Willemot [92]. The state independent statistical factor for this species is 4. There are no state dependent statistical factors for this species. The analytical expression was used throughout the entire temperature range.

The vibrational partition sum was calculated using the vibrational fundamentals of Ref. 34 and are reported in Table 12.

The value for the rotational partition sum at 300K determined in this work is 35756.94, which can be compared with the JPL [15] value of 8883.8, noting that the JPL value neglects the state independent statistical factor of 4.

HO_2

Only the principal isotopic species of the hydroperoxy radical is considered in this study. The rotational partition sum was calculated using the analytical formula of Watson [6] with the rotational constants of Charo and DeLucia [93]. The state independent statistical factor for this species is 2. There are no other state dependent factors for this species. The analytical expression, of Watson, with an additional statistical factor of 2 was in order to account for the *F*-splittings due to ESR present in this open shell molecule, was used throughout the temperature range of the study.

The vibrational partition sum was calculated using the vibrational fundamentals from Norton and Rinsland [34]; ν_1=3436 cm^{-1}, ν_2=1392 cm^{-1}, and ν_3=1098 cm^{-1}.

The JPL catalogue [15] reports a value for the rotational partition sum at 300K of 4 375.703, which compares well with our value of 4 361.59.

O

As the oxygen atom has no defined rotational or vibrational partition sum, it was omitted from this study.

$ClONO_2$

Two species of chlorine nitrate are considered in this study: $^{35}Cl^{16}O^{14}N^{16}O_2$ and $^{37}Cl^{16}O^{14}N^{16}O_2$. The rotational partition sums for both species were calculated using the analytical formula of Watson [6], with the rotational constants of Carten and Lovejoy [94]. The state independent statistical factor is 12 for both species. There are no state dependent statistical factors for either species. The analytical expression was used for both species throughout the entire temperature range.

The vibrational partition sum was calculated using the vibrational fundamentals of Norton and Rinsland [34], with the addition of ν_9 = 122cm-1, which was originally omitted from Ref. 34 as discussed in Ref. 3. The values are presented in Table 13. A complete description of the torsional behavior of this species has not yet been included.

The values of the partition sums obtained in this work compare well with the values from the JPL catalog [15]. The JPL values for the rotational partition sums at 300K, which omit the state independent statistical factor of 12 are 100 540 and 103 108 for the $^{35}Cl^{16}O^{14}N^{16}O_2$ and $^{37}Cl^{16}O^{14}N^{16}O_2$ species respectively, while our values are 1 214 131.37 and 1 245 035.12 respectively. Our total internal partition sums at 296 K, 4 788 793.44 and 4 910 684.51 for $^{35}Cl^{16}O^{14}N^{16}O_2$ and $^{37}Cl^{16}O^{14}N^{16}O_2$, can be compared with the values from Flaud et al. [95] of 4 849 698. and 5 019 571.

NO+

Only the principal isotopic species of NO+ was considered in this study. The rotational partition sum was calculated using McDowell's analytical expression [5], with the rotational constants of von Esse [96]. The state independent statistical factor for this molecule is 3. There are no state dependent statistical factors. The analytical expression was used throughout the temperature range of interest.

The vibrational partition function was calculated using the vibrational fundamental of Ref. 96; 2344 cm^{-1}.

HOBr

Two species of HOBr were considered in this study: $H^{16}O^{79}Br$ and $H^{16}O^{81}Br$. The rotational partition sums for both species were calculated using Watson's analytical expression [6], with the rotational constants of Cohen et al. [97]. The state independent statistical factor is 8 for both species. There are no state dependent statistical factors for either species. The analytical formula was used for both species throughout the entire temperature range of interest.

The vibrational partition sum was calculated using the vibrational fundamentals of Cohen et al. [97] shown in Table 14.

The partition sums calculated for HOBr agree well with the values published in the JPL catalog [15]. Our values of Q_{rot} at 300K are 29 046.34 for the $H^{16}O^{81}Br$ species and 28 987.19 for the $H^{16}O^{79}Br$ species. These values compare favorably with the JPL

values which are 13 611.629 for the $H^{16}O^{81}Br$ species and 13 552.774 for the $H^{16}O^{79}Br$ species, bearing in mind that these values apparently neglect the spin of the hydrogen atom from the state independent degeneracy factor.

C_2H_4

Three isotopomers of C_2H_4 were considered in this study: $^{12}C_2H_4$, $^{12}C^{13}CH_4$ and $^{12}C_2H_3D$. Rotational partition sums for both species were calculated using Watson's analytical formula [6], using the rotational constants of Ref. 98 for the $^{12}C_2H_4$ species, Ref. 99 for the $^{12}C^{13}CH_4$ species and Ref. 100 for the $^{12}C_2H_3D$ species. The state independent degeneracy factors are 1, 2 and 24 for the $^{12}C_2H_4$, $^{12}C^{13}CH_4$ and $^{12}C_2H_3D$ species respectively. The state dependent degeneracy factors are 5 for the even levels and 3 for the odd levels of the non-deuterated species [101]. The deuterated species have no state dependent degeneracy factors. The analytical expression was used for all three species throughout the temperature range.

The vibrational partition functions were calculated using the constants from Norton and Rinsland [34] for the $^{12}C_2H_4$ species and Duncan et al. [102, 103] for the $^{12}C_2H_3D$ species. See Table 15 for the values. The vibrational partition sum for the $^{12}C^{13}CH_4$ species was calculated using the vibrational fundamentals of $^{12}C_2H_4$.

Recall of Data

Although some compilations of partition functions [1, 2. 104, 105] utilized a four- or five-coefficient polynomial fit to the $Q(T)$ data and provided the coefficients as a means of rapid recall, this work has abandoned that concept in favor of interpolation.

The reasons for this transition are numerous. First, as available computer power and storage space constantly increase, it is no longer necessary to provide final data in the most terse manner possible. The entire set of tables as an uncompressed, fixed format file occupies only a few megabytes of storage space, and although the interpolation routines require somewhat more computer time than the polynomial expansion, both methods are nearly instantaneous in modern terms.

Second, when polynomial fits were used, there were a number of species for which the error introduced by the fits was greater than the 1% criterion at certain temperatures. Studies revealed that systems with many low lying vibrational states gave vibrational partition sums that increase rapidly. When the product with the rotational partition sum is made the resulting total internal partition sum increases too rapidly for the polynomial to fit accurate in the chosen temperature ranges. With interpolation of $Q(T)$ data the situation is improved. The values produced by interpolation are, in general, much closer to the calculated values than those produced by polynomial expansion. Fig. 5 shows the error introduced by using interpolation with a step size of 50 K for nitric acid. Nitric acid was selected for this study because its partition function is one of the most difficult species to fit by a polynomial function. As evidenced by these graphs, a step size of 50K is more than satisfactory, even for a species which is troublesome to fit.

A third reason for the switch to interpolation is that it presents the data in the most direct form possible. By looking at the tables, or using them as input data to a graphing

program, it is possible to immediately see trends in the partition functions. Also, since the actual numbers are provided, rather than coefficients which are not directly meaningful, there is a much smaller chance of the wrong values being used in a calculation, or the accidental switching of two coefficients for example.

As part of this work, various interpolation schemes were considered. Since partition functions have a rather exponential trend, the concept of storing either $ln(Q(T))$ versus T or $ln(Q(T))$ versus $ln(T)$ was tested for the efficacy of reducing interpolation errors. Three schemes were tested; 4-point Lagrange interpolation of $Q(T)$ versus T, $ln\{Q(T)\}$ versus T, and $ln\{Q(T)\}$ versus $ln\{T\}$. Figure 6 shows the percent difference (calculated-interpolated) for the three schemes for nitric acid. From the plot it is clear that the $Q(T)$ versus T and $ln\{Q(T)\}$ versus $ln\{T\}$ interpolations are more precise than the $ln\{Q(T)\}$ versus T interpolation. Figure 7 shows the maximum error at all points within the temperature range of interest for nitric acid, for the $Q(T)$ versus T and $ln\{Q(T)\}$ versus $ln\{T\}$ interpolations as a function of the spacing between temperature points. As Fig. 7 shows, although taking the logarithm of both axes significantly reduces the maximum error at large step-size values for most species, it does little, or even increases the error at smaller step-size values. Additionally, providing tables of $ln(Q(T))$ versus $ln(T)$ still makes it impossible to examine the data without performing further calculations. In light of all of these findings, and a critical analysis of the size of the tables required versus induced error, the decision was made to use interpolation with a 25K step size and no logarithms.

Data tables were generated that list values for $Q(T)$ at 25K intervals. A four-point Lagrange interpolation scheme is used, with extra points provided below 70K and above

3000K so that a four point interpolation can be used throughout the entire temperature range. These tables and the four-point Lagrange interpolation scheme were then coded into a FORTRAN program (TIPS_2003.for) and subroutine (BD_TIPS_2003.for) and are available from one of the authors (RRG, see *faculty.uml.edu/Robert_Gamache*) or the HITRAN ftp site (*cfa-ftp.harvard.edu/pub/HITRAN*).

Discussion

The partition sums calculated above include all isotopomers on the HITRAN database as well as some isotopomers not currently on the database. The partition sums are provided in tabular form with a 25K step size, accompanied by a Lagrange interpolation program to evaluate the partition sums at any temperature within the temperature range of this study. The partition sums are also provided in tabular form in 1 K step intervals on the HITRAN website site (*cfa-ftp.harvard.edu/pub/HITRAN*). The conversion to an interpolation scheme has allowed for the rapid distribution of a number of partition sums which were previously undistributed because they could not be fit with a suitable degree of accuracy to the polynomial expression used at that time.

Although this work is similar to previously released partition functions, it also includes many new species, interpolation for greater accuracy and incorporates all of the corrections to the previous set of partition functions discussed in Goldman et al. [3] The partition sums computed here are compared with literature values when available. Most of the comparisons show very good agreement: the percent difference, $100*(Q_{literature}-Q_{this\ work})/Q_{literature}$, for 83 comparisons are less than 1 percent, 14 are between 1 and 2 percent,

and for C_2H_6 at 300 K is 4.75%. There are a number of improvements that will be made to the partition sums in the future. For molecular systems where it is necessary to use the product approximation this work only included the harmonic oscillator approximation of Herzberg [10] for the vibrational partition sums. Anharmonic corrections will be added to the model for ethane. The analytical approximation of the rotational partition sum for asymmetric rotors [6] includes a component for centrifugal distortion that was not applied in this work.

A near complete set of figures used for the study of convergence of the direct sum and analytical partition sums, as well as comparisons between calculations, etc. are available at the web site of one of the authors (*faculty.uml.edu/Robert_Gamache*).

Acknowledgements

The authors would like to acknowledge Alain Barbe for providing constants for rare, isotopically substituted species of ozone. Several of the authors (JF and RRG) are also pleased to acknowledge the support of this research by the National Science Foundation Grants No. ATM-9812540 and ATM-0242537, and the University of Massachusetts Lowell Council on Teaching, Learning and Research as Scholarship. Any opinions, findings, and conclusions or recommendations expressed in this material are those of the author(s) and do not necessarily reflect the views of the National Science Foundation.

References

[1] Gamache RR, Hawkins RL, Rothman LS. Total internal partition sums in the temperature Range 70 - 3000 K: Atmospheric linear molecules. J Mol Spectrosc 1990;142:205-19.

[2] Gamache RR, Kennedy S, Hawkins R, Rothman LS. Total internal partition sums for molecules in the terrestrial atmosphere. J Mol Struct 2000;517-518:413-31.

[3] Goldman A, Gamache RR, Perrin A, Flaud J-M, Rinsland CP, Rothman LS. HITRAN partition functions and weighted transition-moments squared. J Quant Spectrosc Radiat Transfer 2000;66:455-86.

[4] Rothman LS, Barbe A, Benner DC, Brown LR, Camy-Peyret C, Carleer MR, Chance KV, Clerbaux C, Dana V, Devi VM, Fayt A, Fischer J, Flaud J-M, Gamache RR, Goldman A, Jacquemart D, Jucks KW, Lafferty WJ, Mandin J-Y, Massie ST, Newnham DA, Perrin A, Rinsland CP, Schroeder J, Smith KM, Smith MAH, Tang K, Toth RA, Vander-Auwera J, Varanasi P, and Yoshino K. he HITRAN Molecular Spectroscopic Database: Edition of 2000 Including Updates through 2001, J Quant Spectrosc Radiat Transfer 82 (2003) 5–44.

[5] McDowell RS. Rotational partition functions for linear molecules. J Chem Phys 1988;88:356-61.

[6] Watson JKG. The asymptotic asymmetric-top rotational partition function. Mol Phys 1988;65:1377-97

[7] McDowell RS. Centrifugal Distortion Corrections to Calculated Thermodynamic Functions, J Chem Phys 1963;39:526-28.

[8] McDowell RS. Rotational partition functions for spherical-top molecules. J Quant Spectrosc Radiat Transfer 1987;71:414-29.

[9] McDowell RS. Rotational partition functions for symmetric-top molecules. J Chem Phys 1990;93:2801-11.

[10] Herzberg, G, "Molecular Spectra and Molecular Structure II. Infrared and Raman Spectra of Polyatomic Molecules," Van Nostrand, New York, 1960.

[11] Coudert, L, Université Pierre et Marie Curie , private communication, 1993.

[12] Watson JKG. Determination of centrifugal distortion coefficients of Asymmetric- Top molecules. J Chem Phys 1967;46:1935-49.

[13] Flaud, J-M, and Camy-Peyret, C, Université Pierre et Marie Curie, private communication, 1991.

[14] Rothman LS, Gamache RR, Tipping RH, Rinsland CP, Smith MAH, Benner DC, Malathy Devi V, Goldman A, Flaud J-M, Camy-Peyret C, Perrin A, Goldman A, Massie ST, Brown LR, Toth RA. The HITRAN molecular database: Editions of 1991 and 1992. J Quant Spectrosc Radiat Transfer 1992;48:469-507.

[15] Pickett, H.M., Poynter, R.L., Cohen, E.A., Delitsky, M.L., Pearson, J.C., Muller, HSP. Submillimeter, millimeter and microwave spectral line catalog, 1996 ed. Caltech, Pasadena CA: JPL Publication 80-23, Rev. 4.

[16] Flaud J-M, Camy-Peyret C. Vibration-Rotation intensities in H_2O- Type molecules application to the $2\nu_2$, ν_1 ,ν_3 Bands of $H_2{}^{16}O$. J. Mol. Spectrosc 1975;55:278-310

[17] Rothman LS, Hawkins RL Wattson RB, Gamache RR. Energy levels, intensities and linewidths of atmospheric carbon dioxide bands. J Quant Spectrosc Radiat Transfer 1992;48:537-66.

[18] Chedin A, Teffo J-L. The Carbon Dioxide Molecule: A New Derivation of the Potential, Spectroscopic, and Molecular Constants, J Mol Spectrosc 1984;107:333-42.

[19] Gray LD ,Young AT. Relative Intensity Calculations For Carbon Dioxide – IV: Calculations of the Partition Function For Isotopes Of CO_2. J Quant Spectrosc Radiat Transfer 1969;9:569-89.

[20] Flaud J- M, Camy-Peyret C, Devi VM, Rinsland CP, Smith MAH. The ν_1 and ν_2 bands of $^{16}O_3$: line positions and intensities. J Molec Spectrosc 1987;124:209-217.

[21] Flaud J-M, Camy-Peyret C, N'Gom A, Devi VM, Rinsland CP, Smith MAH. The ν_2 bands of $^{16}O^{18}O^{16}O$ and $^{16}O^{16}O^{18}O$: line positions and Intensities. J Molec Spectrosc 1989;133:217-23.

[22] Rinsland CP, Smith MAH, Devi VM, Perrin A, Flaud J-M, Camy- Peyret C. The ν_2 bands of $^{16}O^{17}O^{16}O$ and $^{16}O^{16}O^{17}O$: line positions and Intensities. J Molec Spectrosc 1991;149:474-80.

[23] Barbe, A, Université Reims-Champagne-Ardenne, Private communication, 2001.

[24] Flaud J-M, Camy-Peyret C, Devi VM, Rinsland CP, Smith MAH. The ν_1 and ν_3 bands of $^{16}O^{18}O^{16}O$: line positions and intensities. J Molec Spectrosc 1986;118:334-44.

[25] Camy-Peyret C, Flaud J-M, Perrin A, Devi VM, Rinsland CP, Smith MAH, The hybrid-type bands ν_1 and ν_3 of $^{16}O^{18}O^{16}O$: line positions and intensities. J Molec Spectrosc 1986;118:345-54.

[26] Heyart M, Perrin A, Flaud J-M, Camy-Peyret C, Rinsland CP, Smith MAH, Devi VM. The ν_1 and ν_3 Bands of $^{16}O^{17}O^{16}O$: line Positions and Intensities. J Molec Spectrosc 1992;156:210-216.

[27] Toth RA. Frequency of N_2O in the 1100-to 1440 cm^{-1}. J Opt Soc Am 1986; B3;1263-81.

[28] Gray LD ,Young AT. Note :Calculation of The Partition Function For $^{14}N_2^{16}O$. J Quant Spectrosc Radiat Transfer 1971;11:1265-70.

[29] Guelachvili G, DeVilleneuve D, Farrenq R, Urban W ,Verges J. Dunham Coefficients for Seven Isotopic Species of CO. J Molec Spectrosc 1983;98:64-79.

[30] Tipping, RH, University of Alabama, private communication, 1994.

[31] Tarrago G, Dang-Nhu M, Poussigue G, Guelachvili G, Amiot C. The ground state of methane $^{12}CH_4$ through the forbidden lines of the ν_3 band. J Mol Spectrosc 1975;57:246-63.

[32] Dang-Nhu M, Pine AS, Robiette AG. Spectral intensities in the ν_3 band of $^{12}CH_4$ and $^{13}CH_4$. J Molec Spectrosc 1979;77:57-68.

[33] Tarrago G, DeLaveau M, Fusina L, Guelachvili G. J Absorption of $^{13}CH_4D$ at 6-10μm: Triad ν_3 , ν_5 , ν_6 . J Molec Spectrosc 1987;126:149-58.

[34] Norton RH, Rinsland CP. ATMOS data processing and science analysis methods. Appl Opt 1991;30:389-400.

[35] Robiette AG ,Dang-Nhu M. Rotational partition functions of methane and its isotropic species. J Quant Spectrosc Radiat Transfer 1979;22:499-501.

[36] Gamache RR, Goldman A, Rothman LS. Improved spectral parameters for the three most abundant isotopomers of the oxygen molecule. J Quant Spectrosc Radiat Transfer 1998;59:495-509.

[37] Gamache RR, Goldman A. Einstain A coefficient, integrated band intensity, and population factors: Application to the a $^1\Delta_g - X\,^3\Sigma_g^-$ (O,O) O_2 band J Quant Spectrosc Radiat Transfer 2001;69:389-401.

[38] Ritter KJ, Wilkerson TD. High-Resolution spectroscopy of the Oxygen A Band. J Molec Spectrosc 1987;121:1-19.

[39] Schermaul R. Transition probability and line broadening for the $b^1\sum^+_g$ $(\nu = 0) \leftarrow X^3\sum^+_g (\nu = 0)$ band of the $^{16}O^{18}O$ isotopomer of oxygen . J Quant Spectrosc Radiat Transfer 1999;62:181-91.

[40] Amiot C, Bacis R, Guelachvili G. Infrared study of the $X^2\Pi$ ν=0, 1, 2 levels of $^{14}N^{16}O$. Preliminary results on the n=0,1 levels of $^{14}N^{17}O$, $^{14}N^{18}O$, and $^{15}N^{16}O$. Can J Phys 1978;56:251-65.

[41] Meerts WL. A theoretical reinvestigation of the rotational and hyperfine lambda doubling spectra of diatomic molecules with a $A^2\Pi$ State: The spectrum of NO. Chemical Physics 1976;14:421-25.

[42] Pine AS, Dresselhaus G, Palm B, Davies RW, Clough SA. Analysis of the 4-μm $\nu_1 + \nu_3$ combination band of SO_2. J Mol Spectrosc 1977;67:386-415.

[43] Lafferty WJ, Pine AS, Flaud J-M, Camy-Peyret C. The $2\nu_3$ band of $^{32}S^{16}O_2$: line positions and intensities. J Mol Spectrosc 1993;157:499-511.

[44] Lafferty WJ, Fraser, GT, Pine, AS, Flaud J-M, Camy-Peyret C, Dana V, Mandin, J-Y, Barbe, A. Plateaux, J.J., Bouazza, S. The $3\nu_3$ band of $^{32}S^{16}O_2$ line positions and intensities. J. Molec. Specrosc 1992;154: 51-60.

[45] Chu PM, Wetzel SJ, Lafferty WJ, Perrin A , Flaud J-M, Arcas Ph, Guelachvili G. Line intensities for the 8-μm bands of SO_2. J Mol Spectrosc 1998;189:55-63.

[46] Perrin A, Flaud J-M, Camy-Peyret C, Carli B, Carlotti M. The far infrared spectrum of $^{14}N^{16}O_2$. Electron spin-rotation and hyperfine Fermi contact resonances in the ground state. Mol Phys 1988;63:791-810.

[47] Poynter RL, Margolis JS. The ground state far infrared spectrum of NH_3 . Mol Phys 1983;48:401-18.

[48] Carlotti M, Trombetti A, Velino B, Vrbancich J. The rotation-inversion spectrum of $^{15}NH_3$. J Mol Spectrosc 1980;83:401-7.

[49] Urban Š, Papoušek D, Devi M, Fridovich B, D'Cunha R, Narahari Rao K. Transition dipole matrix elements for $^{14}NH_3$ from the line intensities of the $2\nu_2$ and ν_4 bands . J Mol Spectrosc 1984;106:38-55.

[50] Pine AS, Dang-Nhu M. Spectral intensities in the ν_1 band of NH_3 . JQSRT 1993;50:565-70.

[51] Aroui H, Broquier M, Picard-Bersellini A, Bouanich JP, Chevalier M, Gherissi S. Absorption intensities, pressure-broadening and line mixing parameters of some lines of NH_3 in the ν_4 band. J Quant Spectrosc Radiat Transfer 1998;60:1011-23.

[52] Devi VM, Narahari Rao K, Pracna P, Urban S. Intensities in the ν_4 band of $^{15}NH_3$. J Mol Spectrosc 1990;143:18-24.

[53] Maki, AG, and Wells, JS, High Resolution Spectrum of the n_5 Band of Nitric Acid (HNO_3) near 880 cm^{-1}, J. Molec. Spectrosc. 108 (1984) 17-30.

[54] Maki AG. High Resolution measurements of the ν_2 band of HNO_3 and the ν_3 band of trans-HONO. J Mol Spectrosc 1988;127:104-11.

[55] Beaudet RA, Poynter RL. Mirowave Spectra of Molecules of Astrophysical Interest.XII. Hydroxyl Radical. J Phys Chem Ref. Data 1978;7:311-13.

[56] Tipping RH, Univ. of Alabama, private communication, 1992.

[57] J.A. Coxon and J.F. Ogilvie, "Precise potential-energy function for the $X^1\Sigma^+$ state of hydrogen chloride," J.Chem.Soc.Faraday Trans. II 1982;**78:** 1345-62.

[58] Stocker RN, Goldman A. Infrared spectral line parameters of HBr And DBr at elevated temperatures. J Quant Spectrosc Radiat Transfer 1976;16:335-46.

[59] Guelachvili G, Niay P, Bernage P. Infrared bands of HCl and DCl by Fourier transform spectroscopy Dunham coefficients for HCl, DCl, and TCl. J Molec Spectrosc 1981;85:271-81.

[60] Endo Y, Sato S, Hirota E. Microwave spectroscopy of the CCl radical. J Molec Spectrosc 1982;94:199-207.

[61] Cohen EA, Pickett HM, Geller M. The submillimeter spectrum of ClO. J Molec Spectrosc 1984;106:430-35.

[62] Maki AG. Microwave spectra of molecules of astrophysical interest VI: carbonyl and hydrogen cyanide. J Phys Chem Ref Data 1974;3:221-44.

[63] Hunt N, Foster SC, Johns JWC, McKellar ARW. High-resolution spectroscopy of 16 bands of OCS in the region 1975-2140 cm^{-1} for diode laser calibration. J Mol Spectrosc 1985;111:42-53.

[64] Wells JS, Petersen FR, Maki AG, Sukle DJ. Heterodyne frequency measurements on the 11.6-μm band of OCS: new frequency/wavelength calibration tables for 11.6- and 5.8-μm OCS bands. Appl.Opt.1981;20: 1676-84.

[65] Mürtz M, Palm P, Urban W, Maki AG. More Sub-Doppler Heterodyne Frequency Measurements on OCS between 56 and 63 THz. J Mol Spectrosc 2000; 204: 281-28.

[66] Tan TL, Looi EC, Lee KK. Hot-Band Spectrum of CO_2 near 700 cm^{-1} and the ν_1 Band of $OC^{34}S$. J.Mol.Spectrosc.1993; 157: 261-67.

[67] Brown LR, Fayt A. private communication, 1997.

[68] Bouanich J-P, Blanquet G, Walrand J, Courtoy CP. Diode laser measurements of line strengths and collisional half-widths in the ν_1 band of OCS at 298 K. J Quant Spectrosc Radiat Transfer 1986;36:295-306.

[69] Blanquet G, Walrand J, Hilgers I, Lambot D. Spectral intensities in the ν_1 band of carbonyl sulfide and its isotropic species. J Mol Spectrosc 1990;140:295-300.

[70] Winnewisser G, Cornet RA, Birss FW, Gordon RM, Ramsay DA, Till SM Determination of the ground state rotational constants for formaldehyde: $H_2{}^{12}CO$ and $H_2{}^{13}CO$. J Mol Spectrosc 1979;74:327-9.

[71] Dangoisse D, Willemot E, Bellet J. Microwave spectrum of Formaldehyde and its isotopic species in D, ^{13}C, and ^{18}O: Study of Coriolis resonance between ν_4 and ν_6 vibrational excited states. J Mol Spectrosc 1978;71:414-29.

[72] Lovas FJ, National Institute of Standards and Technology, private communication, 1989.

[73] Reuter D, Jennings DE, Brault JW. $v = 1 \leftarrow 0$ Quadrupole spectrum of N_2. J. Molec. Spectrosc.1986; 115: 294-304.

[74] Di Lauro C, Alamichel C. Rotational analysis of the $\nu_2 + \nu_6^{\pm 1}$, $\nu_5 \mp + \nu_6^{\pm 1}$,and $2\nu_3 + \nu_6^{\pm 1}$ Interacting Infrared Bands of Methyl Chloride. J Molec Spectrosc 1980;81:390- 412.

[75] Blanquet C, Walrand J, Dang-Nhu M. Absolute line intensities of the ν_6 band of $CH_3{}^{35}C1$ at 10 μm. J Molec Spectrosc 1993;159:156-60.

[76] Blanquet G, Warland J, Dang-Nhu M. Spectral intensities in the ν_3 band of $^{12}CH_3$. J Molec Spectrosc.1989;133:471-74.

[77] Dang-Nhu M, Blanquet C, Warland J, Derie F. Spectral intensities in the ν_3-band of $^{12}C11_3{}^{35}C1$ at 13μm. Molecular Physics 1988;65:77-833.

[78] Flaud J-M, Camy-Peyret C, Johns JWC, Carli B. The far infrared spectrum of H_2O_2. First observation of staggering of the levels and determination of the *cis* barrier. J Chem Phys. 1989;91:150-51.

[79] Perrin A, Flaud J-M, Camy-Peyret C, Schernaul R, Winnewisser M, Mandin J-Y, Dana V, Badaoui M, Koput J. Line intensities in the far infrared spectrum of H_2O_2. J Molec Spectrosc 1996;176:287-96.

[80] Flaud J-M, Perrin A. High-resolution infrared spectroscopy and one dimensional large amplitude motion in asymmetric tops: HNO_3 and H_2O_2. Chap. 7 in *Vibration-Rotational Spectroscopy & Molecular Dynamics,* pp. 39~ 460, in Advanced Series in Physical Chemistry - Vol.9, D. Papousek, editor, World Scientific Publishing Co., Singapore, 1997.

[81] Klee S, Winnewisser M, Perrin A, Flaud J-M. Absolute line intensities for the ν_6 band of H_2O_2. J Molec Spectrosc 1999; 195:154-61.

[82] Hietanen J, Kauppinen J. High- Resolution infrared spectrum of acetylene in the region of the bending fundamental ν_5. Molecular Physics 1981;42:411-423.

[83] Duncan JL, McKean DC, Bruce AJ. Infrared spectroscopic studies of partially deuterated ethane. J. Molec. Spectrosc 1979;74:361-74.

[84] Pine AS, Rinsland CP. The role of torsional hot bands in modeling atmospheric ethane . J Quant Spectrosc Radiat Transfer 1999;62 445-58.

[85] Maki AG, Sams RL, Olsen WB. Infrared determination of C_0 for phosphine via perturbation- allowed $\Delta|k\text{-}l| = \pm 3$ transitions in the $3\nu_2$ band. J Chem Phys 1973;58:4502-12.

[86] Tarrago G, Dang-Nhu M, Goldman A. Analysis of Phosphine Absorption in the region 9-10 μm and High-Resolution Line-by-Line Simulation of the ν_2 and ν_4 Bands. J Molec Spectrosc 1981; 88:311-22.

[87] Baldacci A, Devi VM, Rao KN, Tarrago G. Spectrum of Phosphine at 4-5 mm: Analysis of the ν_1 and ν_3 Bands. J Molec Spectrosc 1980; 81:179-206.

[88] Goldman A, Rinsland CP, Blatherwick RD, Bonomo FS. Spectroscopic line parameters for the ν_6 band of carbonyl fluoride. Appl Opt 1990;29:1860-3.

[89] Bobin B, Borde CJ, Borde J, Breant C. Vibrational-rotational molecular constants for the ground and ν_3 =1 states of $^{32}SF_6$ from saturated option spectroscopy. J Mol Spectrosc 1987;121: 91-127

[90] Pine AS, Patterson CW. Doppler-limited spectrum and analysis of the $2\nu_1 + \nu_3$ bands of SF_6 . J, Mol. Spectrosc 1982;92: 18-32.

[91] Flaud JM, Camy-Peyret C, Johns JWC. The far infrared spectrum of hydrogen sulphide. The (0 0 0) rotational constants of $H_2{}^{32}S$, $H_2{}^{33}S$ and $H_2{}^{34}S$. Can J Phys 1983;61:1462-73.

[92] Willemot E. Vibration-rotation Hamiltonian for asymmetric C_s molecules adapted to very strong Coriolis resonance. Applications to the microwave reinvestigations of ν_7 and ν_9 states of $H^{12}COOH$ and $D^{12}COOH$. J Mol Spectrosc 1986;120:246-75

[93] Charo A, DeLucia FC. The millimeter and submillimeter of HO_2 : the effect of unpaired electronic spin in a light assymetric rotor. J Mol Spectrosc 1982;94:426-36.

[94] Carten KP, Lovejoy RW. Modeling the chlorine nitrate ν_4 vibration-rotation band. J. Quant. Spectrosc. Radiat. Transfer 1991;46; 513-17.

[95] Flaud J-M, Orphal J, Lafferty WJ, Birk M, Wagner G. High-resolution vib-rotational analysis of the ν_3 and ν_4 spectral regions of chlorine nitrate. J Geophys Res 2002;12:24-.

[96] von Esse F, Air Force Geophysics Directorate, private communication, 1994.

[97] Cohen E., Jet Propulsion Laboratory, Pasadena CA, private communication, 2002.

[98] Tan TL, Lau SY, Ong PP, Goh KL, Teo HH . High-Resolution Fourier Transform Infrared Spectrum of the ν_{12} Fundamental Band of Ethylene (C_2H_4). J Mol Spectrosc 2000;203:310-313.

[99] De Vleeschouwer M, Lambeau C, Van Lerberghe D, Janssens E, Fayt A. Absorption Spectroscopy of Ethylene $H_2{}^{12}C^{13}CH_2$ in the 4500-cm^{-1} Region. J Mol Spec 1981; 90:273-86.

[100] Herbin P, Blanquet G, Valentin A. Vibration-Rotation Analysis of C_2H_3D from 725-1170 cm^{-1}. J Mol Spec 1988;127:390-98.

[101] Wilson EB Jr. The Stastistical Weights of the Rotational Levels of Polyatomic Molecules, Including Methane, Ammonia, Benzene, Cyclopropane and Ethylene. J Chem Phys 1935;3:276-85.

[102] Duncan JL, Ferguson AM, Goodlad ST. Local mode interpretation of the CH and CD stretching vibrational manifolds of isotopic ethylenes, C_2H_3D and C_2HD_3 . Spectro Chem Acta 1993;49:149-60.

[103] Duncan JL, McKean DC, Mallinson PD, Infrared Crystal Spectra of C_2H_4, C_2D_4, and *as*-$C_2H_2D_2$ and the General Harmonic Force Field of Ethylene. J Mol Spec 1973;45:221-46.

[104] Fischer J, Gamache RR. Total Internal Partition Sums for Molecules of Astrophysical Interest. J Quant Spectrosc Radiat Transfer 2001;74:263-73.

[105] Fischer J, Gamache RR. Partition Sums for Non-Local Thermodynamic Equilibrium Applications. J Quant Spectrosc Radiat Transfer 2001;74:273-84.

Tables

Table 1. Vibrational Fundamentals in cm^{-1} for Water Vapor Isotopologues

	$H_2{}^{16}O$	$H_2{}^{18}O$	$H_2{}^{17}O$	$HD^{16}O$	$HD^{18}O$	$HD^{17}O$
ν_1	3657.053	3649.685	3653.143	2723.680	2723.680*	2723.680*
ν_2	1594.750	1588.279	1591.325	1403.484	1396.2665	1399.6747
ν_3	3755.929	3741.567	3748.318	3707.459	3707.459*	3707.459*

* values from the corresponding band of $HD^{16}O$

Table 2. Vibrational Fundamentals in cm^{-1} for Carbon Dioxide Isotopologues

	$^{12}C^{16}O_2$	$^{13}C^{16}O_2$	$^{12}C^{16}O^{18}O$	$^{12}C^{16}O^{17}O$	$^{13}C^{16}O^{18}O$
ν_1	1388.186 70	1370.0699	1365.828 10	1376.028	1342.293
ν_2 (2 fold degenerate)	667.360 50	648.4645	662.3501	664.730	643.328
ν_3	2349.1650	2283.5217	2332.1363	2340.014	2265.985
	$^{13}C^{16}O^{17}O$	$^{12}C^{18}O_2$	$^{12}C^{17}O^{18}O$	$^{12}C^{16}O_2$	
ν_1	1355.117	1347.098	1355.658	1364.940	
ν_2 (2 fold degenerate)	645.754	657.331	659.704	662.066	
ν_3	2274.100	2314.051	2322.436	2330.593	

Table 3 State-dependent and State-independent Degeneracy Factors for the Isotopologues /Isotopomers of Ozone.

Isotopologues/Isotopomer	g_s		g_i
	Even	odd	
$^{16}O^{16}O^{16}O$	1	0	1
$^{16}O^{16}O^{18}O$	1	1	1
$^{16}O^{18}O^{16}O$	1	0	1
$^{16}O^{16}O^{17}O$	1	1	6
$^{16}O^{17}O^{16}O$	1	0	6
$^{18}O^{18}O^{16}O$	1	1	1
$^{18}O^{16}O^{18}O$	1	0	1
$^{16}O^{17}O^{18}O$	1	1	6
$^{17}O^{16}O^{18}O$	1	1	6
$^{17}O^{18}O^{16}O$	1	1	6
$^{17}O^{17}O^{16}O$	1	1	36
$^{17}O^{16}O^{17}O$	15	21	1
$^{18}O^{18}O^{18}O$	1	0	1
$^{18}O^{18}O^{17}O$	1	1	6
$^{18}O^{17}O^{18}O$	1	0	6
$^{17}O^{17}O^{18}O$	1	1	36
$^{17}O^{18}O^{17}O$	15	21	1
$^{17}O^{17}O^{17}O$	15	21	6

Table 4. Vibrational Fundamentals in cm^{-1} for Ozone Isotopologues/Isotopomers

	$^{16}O_3$	$^{16}O^{16}O^{18}O$	$^{16}O^{18}O^{16}O$	$^{18}O^{18}O^{16}O$	$^{18}O^{16}O^{18}O$	$^{18}O^{18}O^{18}O$
ν_1	700.931	684. 613	693.306	677.504	668.085	661.492
ν_2	1042.084	1028.112	1008.453	993.927	1019.350	984.819
ν_3	1103.137	1090.354	1074.308	1060.709	1072.217	1041.556
	$^{16}O^{16}O^{17}O$	$^{16}O^{17}O^{16}O$	$^{17}O^{17}O^{16}O$	$^{17}O^{16}O^{17}O$	$^{17}O_3$	$^{17}O^{17}O^{18}O$
ν_1	692.435	697.079	688.8	684.0	680.2	672.4
ν_2	1035.358	1024.395	1017.5	1030.5	1012.163	1005.4
ν_3	1095.693	1087.829	1080.2	1086.9	1070.946	1063.7
	$^{17}O^{18}O^{17}O$	$^{18}O^{18}O^{17}O$	$^{18}O^{17}O^{18}O$	$^{17}O^{16}O^{18}O$	$^{16}O^{17}O^{18}O$	$^{16}O^{18}O^{17}O$
ν_1	676.6	668.9	664.5	676.0	680.9	685.0
ν_2	995.1	988.5	1000.3	1024.1	1009.6	1000.8
ν_3	1056.3	1049.1	1055.2	1080.1	1074.7	1066.1

Table 5. Vibrational Fundamentals in cm^{-1} for N_2O Isotopologues

	$^{14}N_2{}^{16}O$	$^{14}N^{15}N^{16}O$	$^{15}N^{14}N^{16}O$	$^{14}N_2{}^{18}O$	$^{14}N_2{}^{17}O$
ν_1	2223.7568	2177.6568	2201.6053	2216.7112	2220.0753
ν_2 (2-fold degenerate)	588.7688	575. 4336	585.3121	584.2247	586.3620
ν_3	1284.9033	1280.3541	1269.8920	1246.8846	1264.7043

Table 6. Vibrational Fundamentals in cm^{-1} for Carbon Monoxide Isotopologues

	$^{12}C^{16}O$	$^{12}C^{17}O$	$^{12}C^{18}O$	$^{13}C^{16}O$	$^{13}C^{17}O$	$^{13}C^{18}O$
ν_1	2143.271 461	2116.295 334	2092.122 010	2096.067 229	Same as principal species	2043.692 206

Table 7. Vibrational Fundamentals in cm^{-1} for Nitric Acid

	$H^{14}N^{16}O_3$
ν_1	3550
ν_2	1710
ν_3	1326
ν_4	1303
ν_5	879
ν_6	647
ν_7	579
ν_8	762
ν_9	458

Table 8. Vibrational Fundamentals in cm^{-1} for OCS Isotopologues

	$^{16}O^{12}C^{32}S$	$^{16}O^{12}C^{34}S$	$^{16}O^{13}C^{32}S$	$^{16}O^{12}C^{33}S$	$^{18}O^{12}C^{32}S$
ν_1	858.9669	847.7394	854.467	853.20	844.
ν_2 (2-fold degenerate)	520. 4221	519.696	505.011	520.04	511.
ν_3	2062.201 19	2061.445 64	2009.228 49	2061.808 36	2026.147 01

Table 9. Vibrational Fundamentals in cm^{-1} for HCN Isotopologues

	$H^{12}C^{14}N$	$H^{13}C^{14}N$	$H^{12}C^{15}N$
ν_1	2097.	2086.	2061.345
ν_2 (2-fold degenerate)	713.0	709.	704.656
ν_3	3311.	3310.5	3310.088

Table 10. Measured and Calculated Energies for as a function of τ and n for H_2O_2.

τ	1	1	2	2	τ 1 and 2
n	$E(\tau,n)_{calculated}$	$E(\tau,n)_{measured}$	$E(\tau,n)_{calculated}$	$E(\tau,n)_{measured}$	$E(\tau,n)_{average}$
0	$-0.781\ 614\ 58\times10^{-4}$	0.00000	$-0.138\ 803\ 11\times10^{-3}$	0.00000	0.0
1	$0.254\ 570\ 66\times10^{3}$	254.5499	$0.254\ 570\ 64\times10^{3}$	254.5499	254.5499
2	$0.569\ 695\ 90\times10^{3}$	569.7427	$0.569\ 696\ 79\times10^{3}$	569.7442	569.74345
3	$0.100\ 094\ 09\times10^{4}$	1000.882	$0.100\ 092\ 57\times10^{4}$	1000.930	1000.906
4	$0.147\ 482\ 54\times10^{4}$	---	$0.147\ 560\ 12\times10^{4}$	---	1475.2133
5	$0.194\ 885\ 14\times10^{4}$	---	$0.196\ 008\ 83\times10^{4}$	---	1954.469 85
6	$0.234\ 737\ 89\times10^{4}$	---	$0.244\ 901\ 98\times10^{4}$	---	2398.199 35
7	$0.273\ 083\ 66\times10^{4}$	---	$0.297\ 546\ 21\times10^{4}$	---	2853.149 35
τ	3	3	4	4	τ 3 and 4
n	$E(\tau,n)_{calculated}$	$E(\tau,n)_{measured}$	$E(\tau,n)_{calculated}$	$E(\tau,n)_{measured}$	$E(\tau,n)_{average}$
0	$0.114\ 475\ 71\times10^{2}$	11.4372	$0.114\ 475\ 60\times10^{2}$	11.4372	11.4372
1	$0.370\ 866\ 60\times10^{3}$	370.8932	$0.370\ 866\ 60\times10^{3}$	370.8932	370.8932
2	$0.776\ 193\ 40\times10^{3}$	766.1148	$0.776\ 199\ 90\times10^{3}$	766.1215	766.11815
3	$0.123\ 510\ 88\times10^{4}$	---	$0.123\ 522\ 66\times10^{4}$	---	1235.1677
4	$0.171\ 477\ 83\times10^{4}$	---	$0.171\ 805\ 62\times10^{4}$	---	1716.417 25
5	$0.215\ 987\ 69\times10^{4}$	---	$0.220\ 110\ 44\times10^{4}$	---	2180.490 65
6	$0.252\ 152\ 67\times10^{4}$	---	$0.270\ 0877\ 2\times10^{4}$	---	2611.2000
7	$0.298\ 295\ 10\times10^{4}$	---	$0.326\ 630\ 09\times10^{4}$	---	3124.625 95

Table 11. Vibrational Fundamentals in cm^{-1} for C_2H_6

$^{12}C_2H_6$	ω / cm^{-1}
ν_1	2954.
ν_2	1388.
ν_3	995.
ν_4	303.
ν_5	2896.
ν_6	1379.
ν_7 (2-fold degenerate)	2985.
ν_8 (2-fold degenerate)	1472.
ν_9 (2-fold degenerate)	822.
ν_{10} (2-fold degenerate)	2969.
ν_{11} (2-fold degenerate)	1468.
ν_{12} (2-fold degenerate)	1190.

Table 12. Vibrational Fundamentals in cm^{-1} for HCOOH

$H^{12}C^{16}O^{16}OH$	ω / cm^{-1}
ν_1	3570.
ν_2	2943.
ν_3	1770.
ν_4	1387.
ν_5	1229.
ν_6	1105.
ν_7	625.
ν_8	1033.
ν_9	638.

Table 13. Vibrational Fundamentals in cm^{-1} for $ClONO_2$

$^{35}Cl^{16}O^{14}N^{16}O_2$ and $^{37}Cl^{16}O^{14}N^{16}O_2$	ω / cm^{-1}
ν_1	1735.
ν_2	1292.
ν_3	809.
ν_4	780.
ν_5	560.
ν_6	434.
ν_7	270.
ν_8	711.
ν_9	122.

Table 14. Vibrational Fundamentals in cm^{-1} for HOBr Isotopologues

	ω / cm^{-1}($H^{16}O^{79}Br$)	ω / cm^{-1} ($H^{16}O^{81}Br$)
ν_1	3614.902	3614.903
ν_2	1162.570 388	1162.494 439
ν_3	620.18	619.05

Table 15. Vibrational Fundamentals in cm^{-1} for C_2H_4 Isotopologues

	ω / cm^{-1} ($^{12}C_2H_4$)	ω / cm^{-1} ($^{12}C_2H_3D$)
ν_1	3026.	3028.2
ν_2	1623.	1605.5
ν_3	1342.	1288.0
ν_4	1023.	1000.
ν_5	3103.	3061.6
ν_6	1236.	1129.
ν_7	949.	808.
ν_8	943.	943.
ν_9	3106.	3096.1
ν_{10}	826.	730.
ν_{11}	2989.	2274.0
ν_{12}	1444.	1400.0

Figures

Figures

1 Comparison of the product approximation, $Q_{vib}*Q_{rot}$, with $Q_{Direct\ Sum}$ for CO_2.

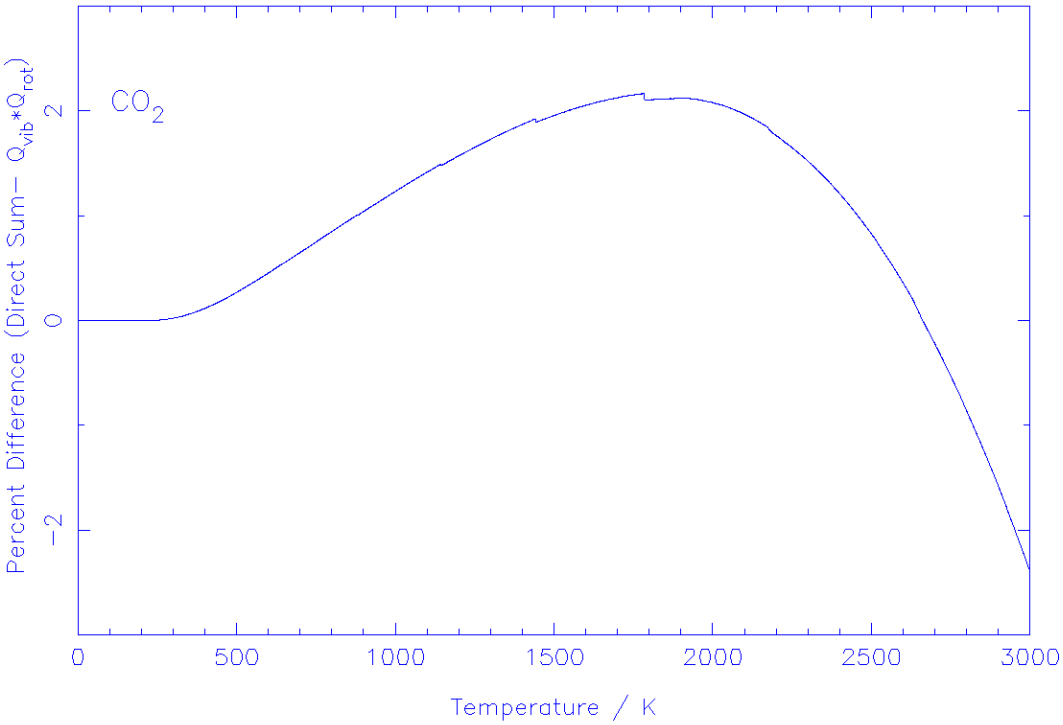

2 Percent difference between $Q_{\text{Direct Sum}}$ and $Q_{\text{analytical formula}}$ for $H_2{}^{16}O$.

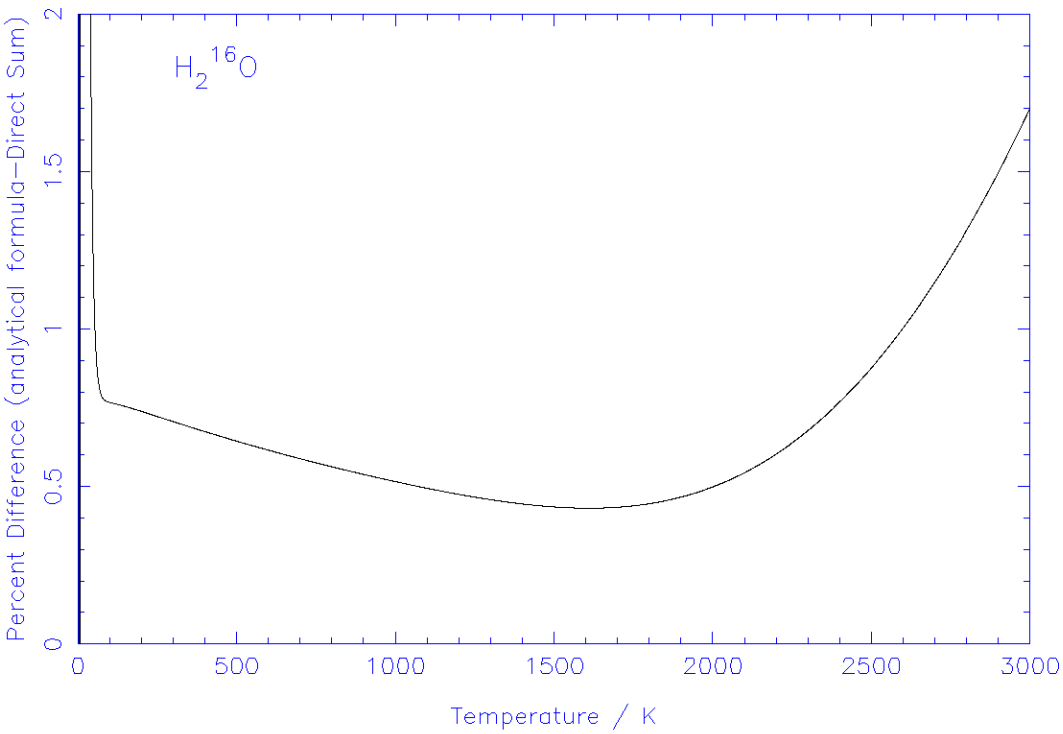

3 Convergence of the partition sum as a function of temperature for $^{16}O_3$.

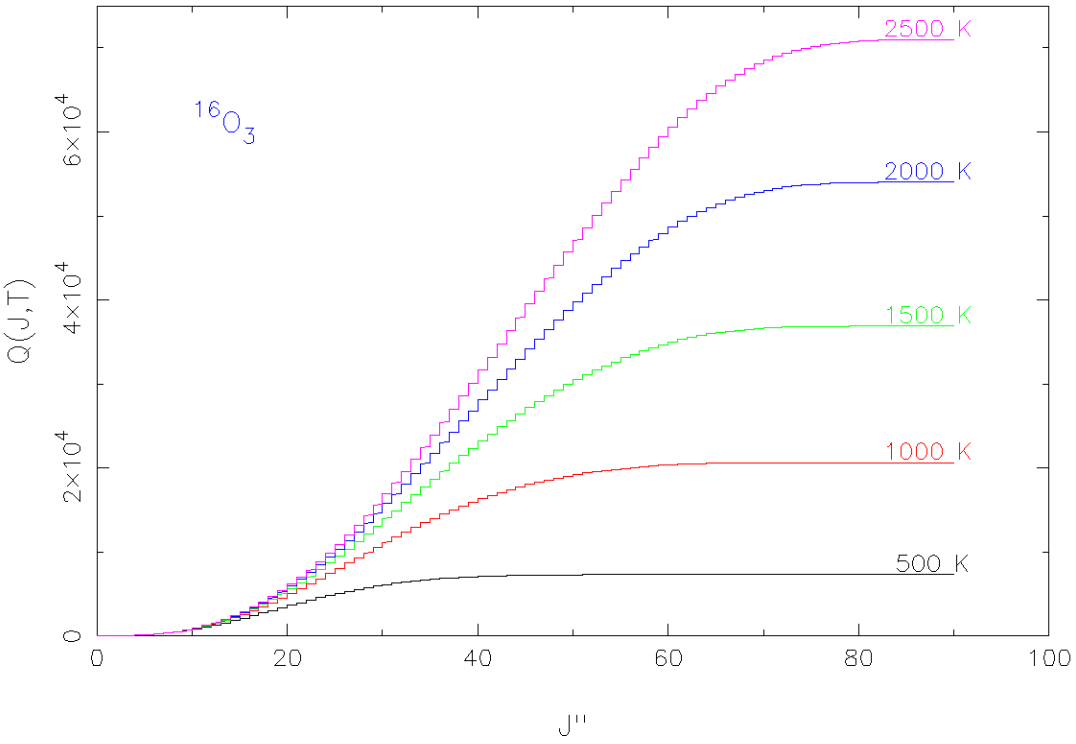

4 Percent difference between $Q_{analytical\ model}$ and $Q_{Direct\ Sum}$ versus temperature for H_2O_2.

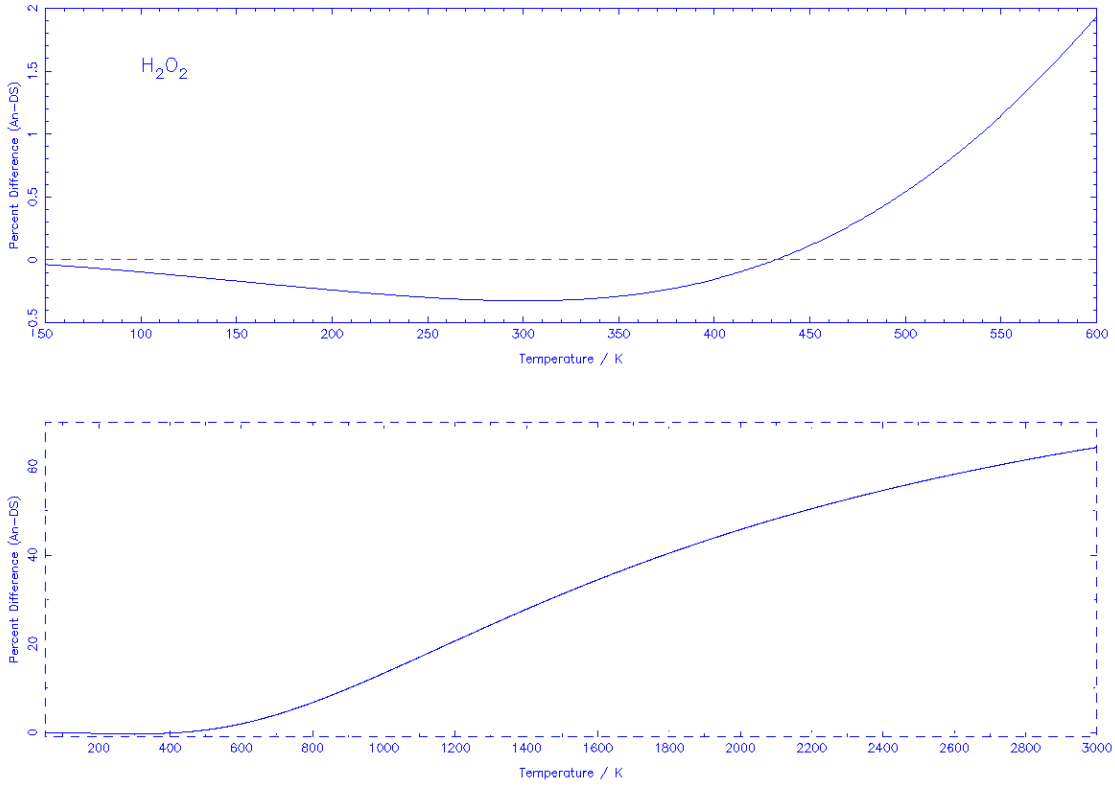

5 Error in recalculated Q(T) by interpolation with 50 K step size for Nitric Acid.

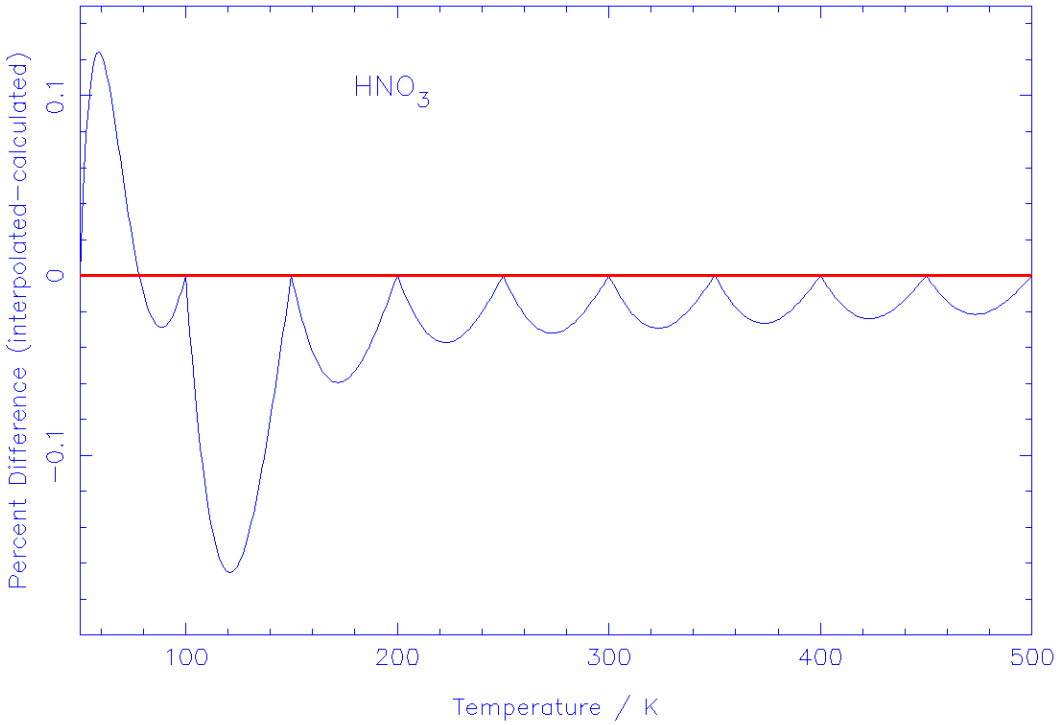

6 Error in recalculated Q(T) by different interpolation schemes with 25 K step size for Nitric Acid. a) Q vs. T, b) ln{Q} vs. T, and c) ln{Q} vs. ln{T}.

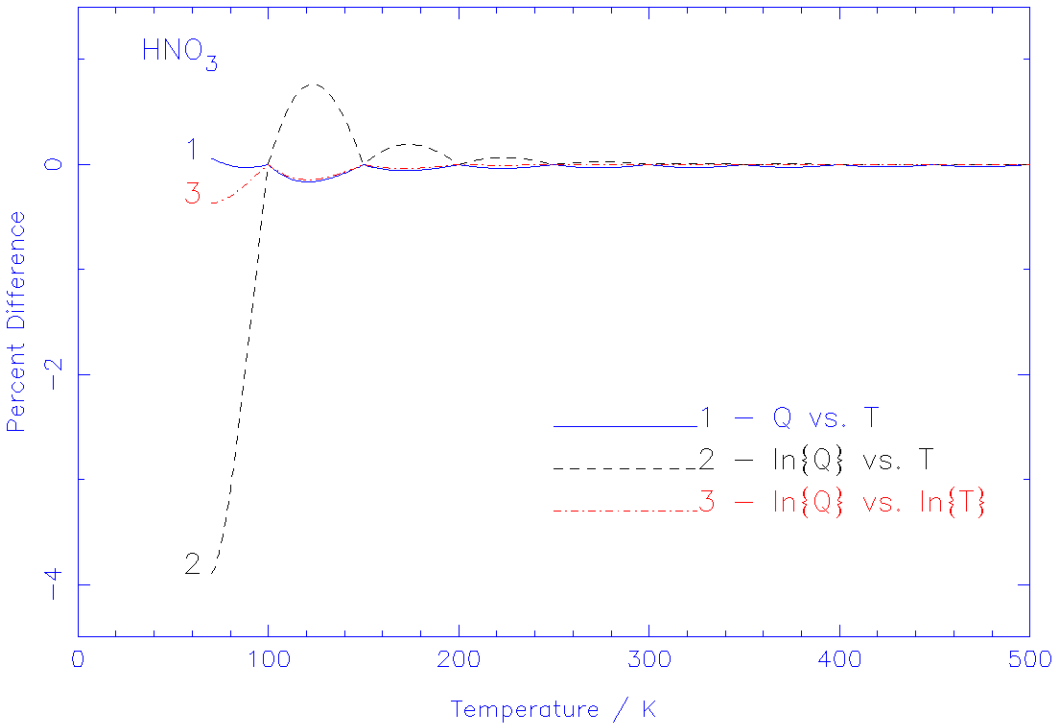

7 Error versus temperature step size in interpolation for Q(T) vs. T (solid circles) and ln{Q(T)} vs. ln{T} (inverted triangles) for Nitric Acid.